

# NASA CONTRACTOR REPORT



NASA CR-1119



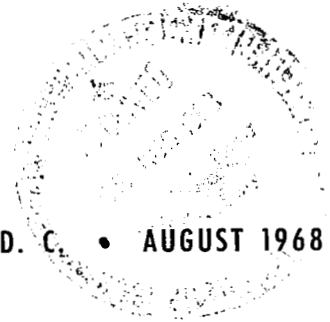
NASA CR-11119

LOAN COPY: RETURN TO  
AFWL (WLIL-2)  
KIRTLAND AFB, N MEX

## DIGITAL PROGRAM FOR DYNAMICS OF NON-RIGID GRAVITY GRADIENT SATELLITES

*by James L. Farrell, James K. Newton, and James J. Connelly*

*Prepared by*  
WESTINGHOUSE ELECTRIC CORPORATION  
Baltimore, Md.  
*for Goddard Space Flight Center*



NATIONAL AERONAUTICS AND SPACE ADMINISTRATION • WASHINGTON, D. C. • AUGUST 1968

NASA CR-1119

TECH LIBRARY KAFB, NM



0060379

DIGITAL PROGRAM FOR DYNAMICS OF NON-RIGID  
GRAVITY GRADIENT SATELLITES

By James L. Farrell,  
James K. Newton, and  
James J. Connelly

Distribution of this report is provided in the interest of information exchange. Responsibility for the contents resides in the author or organization that prepared it.

Prepared under Contract No. NAS 5-9753-10 by  
WESTINGHOUSE ELECTRIC CORPORATION  
Baltimore, Md.

for Goddard Space Flight Center

NATIONAL AERONAUTICS AND SPACE ADMINISTRATION

---

For sale by the Clearinghouse for Federal Scientific and Technical Information  
Springfield, Virginia 22151 - CFSTI price \$3.00



## ABSTRACT

A digital program has been written to determine the dynamic behavior of discretized models for gravity gradient satellite structures. Both passive (elastic reaction, damping) and active (controller) internal torques can be included in the computational model. The program can be utilized simply by observing straightforward directions given in the introductory section of this report, and a concrete example (hinged assembly model of the Radio Astronomy Explorer satellite) of program adaptation is described in detail. To facilitate application to other configurations a clear separation is made between 1) computations applicable to a general gravity gradient satellite, and 2) specific RAE computations.

The basis for this digital program is the Roberson-Wittenburg dynamical formalism, noted and referenced in the text. This formalism grew from the desire to systematize the rigorous dynamic analysis of structures with multiple interconnected members. In programming the formulation for the present problem, it was found possible to supply additional details applicable to a fairly general class of gravity gradient satellites. Thus the general portion of the program contains provisions for straightforward implementation of internal moments (passive spring and damper or active controller torques inherently provided as simple functions of integrated rates and attitude; constraint torques at locked hinge axes automatically accounted for by a simple indexing scheme), as well as solar radiation pressure and thermal (direct Earth and direct plus reflected solar heating) effects. The necessary astronomical and kinematical expressions are supplied in a standard form, with explicit relations valid for eccentricities up to one-tenth.

Practical implementation of the dynamical formalism calls for the following computational refinements: 1) artificial enlargement of small members, to hasten the integration of high frequency oscillations without materially affecting the overall (low frequency) excursions; 2) hinge interactions to enhance the accuracy of numerical differentiation, necessitated by moment characterization for discretized elastic members; 3) the use of weak restraining springs and dampers at locked joint axes, to counteract the double integration of small numerical errors incurred by the constraint torque formulation; 4) representation of torsionless biaxial bending by an orthogonal matrix with one vanishing eigenvector component; and 5) the use of kinetic or potential energy considerations in fitting segments to an elastic curve.

Through successful comparison with an independent Lagrangian model analysis, a three-segment model was deemed sufficient for each of the 750 ft.  $\frac{1}{2}$  inch dia. RAE antenna booms. Each orbit (approximately 4 hours) of the undisturbed satellite then requires roughly one hour of simulation time, and the machine time is approximately doubled by introduction of thermal effects (solar pressure has a less pronounced effect). The expensive nature of the program is attributed to modeling accuracy (e.g., full nonlinear coupling; the interaction between dynamical behavior and forcing functions; etc.) plus the large number of integrated variables, in comparison with the number of independent co-ordinates.



## FOREWORD

This program was written for use by Goddard Space Flight Center, in the dynamic analysis of the Radio Astronomy Explorer satellite, under NASA Contract No. NAS5-9753-10. In combination with additional work performed under this contract (tasks 15 and 20), the results will provide (1) maximum insight into the three-dimensional flexible satellite motion, (2) comparison between this segmented model dynamics and another independent structural analysis (a Lagrangian modal analysis, documented separately), and (3) complete preparation for an operational program which provides statistical filtering of boom tip information (intermittently received by TV stations at fixed points on the Earth) in combination with attitude and damper position measurements.



TABLE OF CONTENTS

<u>Section</u>	<u>Page</u>
INTRODUCTION . . . . .	1
GENERAL PROGRAM COMPUTATIONS . . . . .	7
APPENDIX . . . . .	11
APPENDIX A: ANALYTICAL FORMULATIONS APPLICABLE TO THE GENERAL PROGRAM . . . . .	13
<u>Hinge Torques</u> . . . . .	13
<u>Thermal Bending</u> . . . . .	16
<u>Constraint Torques at Locked Joints</u> . . . . .	21
<u>Radiation Pressure</u> . . . . .	24
<u>Kinematics</u> . . . . .	27
<u>Astronomical Geometry</u> . . . . .	28
APPENDIX B: THE RADIO ASTRONOMY EXPLORER (RAE) SATELLITE CONFIGURATION AND PARAMETERS . . . . .	30
RAE VARIABLE INPUTS (PART I) . . . . .	33
<u>System Parameters</u> . . . . .	33
<u>Initial and Final Conditions</u> . . . . .	34
<u>Astronomical Parameters</u> . . . . .	34
RAE FIXED AND DERIVED INPUTS (PART II) . . . . .	35
<u>Hub and Boom Parameters</u> . . . . .	35
<u>Equilibrium Parameters</u> . . . . .	36
<u>Astronomical Parameters</u> . . . . .	36
<u>General Program Inputs</u> . . . . .	37



TABLE OF CONTENTS (con't)

<u>Section</u>	<u>Page</u>
HYSTERESIS DAMPER SIMULATION . . . . .	48
RAE READOUT DERIVATIONS AND FORMATS . . . . .	49
<u>Constant Readouts</u> . . . . .	49
<u>Variable Readouts</u> . . . . .	49
APPENDIX C: PROGRAM LISTING . . . . .	53
REFERENCES . . . . .	91

## INTRODUCTION

Accurate three-dimensional analysis of non-rigid assemblies has enjoyed only limited feasibility and flexibility in the past, due to the existence of unknown internal forces and moments which influence the relative motion between members. In many applications these relative motions interact with the rigid body degrees of freedom (e.g., the flexural behavior of a satellite boom changes the moments of inertia which in turn affect the attitude dynamics). Because of the resulting complexity, previous investigations have often employed analytical transformations whose detailed form depended heavily upon the specific configuration studied.

In order to provide a method applicable to a more general class of dynamical situations (e.g., flexural and torsional behavior of discretized structural models; attitude control of a hinged satellite assembly), a two-body Euler formulation devised by Fletcher, Rongved, and Yu<sup>1</sup> was extended to the N-body case by Hooker and Margulies;<sup>2</sup> the explicit development was then advanced by Roberson and Wittenberg.<sup>3</sup> These recent advances have been employed in a digital program capable of describing the rotational dynamics (attitude matrices and inertial angular rates) of multiple interconnected rigid bodies. The program is applicable to structural or attitude control problems subject to the conditions (1) existence of a unique path between any pair of bodies (the arrangement then conforms to the definition of a topological "tree"), and (2) characterization of interconnections by hinges which, for any pair of adjacent bodies, must be fixed in both members.

The present scope is restricted to gravity gradient satellites in a Keplerian orbit with eccentricity less than 0.1. In addition to the effects of ellipticity on gravity gradient torque, the program includes solar radiation pressure

(at 100% reflectivity) and thermal bending of booms; heat flux sources are the sun and Earth (direct), plus the component of solar heat reflected by the Earth.

For a reasonably general class of satellites falling within the above scope, the program lends itself quite readily to implementation of accurate dynamic analysis. Although the pertinent mathematical developments (derivations in Refs. 2 and 3, augmented by the additions in Appendix A of this report) involve several arrays of variables, techniques for computer storage optimization have produced a practical computational arrangement for structures containing up to 26 members.\* Aside from a few possible adjustments involving specific satellite geometry,\*\* all that is necessary for immediate use of the program is a specification of the familiar satellite parameters, listed together with the corresponding Fortran designations in quotes below; (Appendix B demonstrates this specification procedure for an illustrative model of the Radio Astronomy Explorer (RAE) satellite;<sup>4</sup> the explicit thoroughness of the Roberson-Wittenburg<sup>3</sup> formulation is attested by the extreme simplicity of these parameters):

System Parameters

$N$  ("N") The number of rigid bodies in the system (There are then  $N-1$  hinges).

$M$  ("EM") A vector ( $N \times 1$ ) defining the mass of each body.

\*To exemplify the demand for machine capacity it is noted that, with 26 members, the augmented inertia matrix of Ref. 3 has  $(26 \times 3)^2$ , or over 6000, elements. This alone consumes about twenty per cent of the IBM 7094 core (the program is written in single precision).

\*\* If solar pressure and/or thermal effects are to be taken into account ( $A_E \neq 0$ ,  $J_E \neq 0$ , or  $J_S \neq 0$ ), see Appendix C.

Also, if formulations of curvature (for hinge moments of discretized booms) require accurate numerical derivatives, the "interacting joint" technique exemplified in Appendix B must be used.

- I ("A") A third order tensor ( $N \times 3 \times 3$ ) containing the principal moments of inertia for each body. (The off-diagonal terms, though initially zero, will be appropriately augmented in accordance with the dynamics in the program).
- R ("R") A third order tensor ( $(N-1) \times 3 \times 3$ ) of restraining torque coefficients which generate position feedback (for control problems) or elastic reaction (for structural analysis) at each hinge.
- R' ("RP") A third order tensor ( $(N-1) \times 3 \times 3$ ) similar to R, but generating hinge torques proportional to relative angular rates between each pair of adjacent bodies.
- S ("S") A matrix ( $N \times (N-1)$ ) of ones and zeros constructed simply as follows: Number the bodies (1 to N) and the hinges (1 to  $N-1$ ). Set  $S_{ij}$  to zero for every combination of unconnected body (i) and hinge (j). For each pair of adjacent members (I and K) identify the one (body I) to which the coefficients R and R' are referenced.\* Set  $S_{IJ}$  to +1 and  $S_{KJ}$  to -1 (where J is the hinge connecting the I and K members).
- P ("RHO") A third order tensor ( $(N-1) \times 3 \times 3$ ) defining the orthogonal transformation between each pair of adjacent body principal axes in the undeformed or rest position. In the notation of the preceding item,  $[P_j]$  is the transformation from K to I co-ordinates.

\*One example requiring such an identification would be a skewed boom hinged to a satellite hub. The rotational degrees of freedom of the hinge would presumably be referenced to principal axes of the boom (bending and torsion), rather than the hub.

- $C$  ("C") A matrix ( $3N \times 3N$ ) generated from  $S$  as follows: All elements outside the upper left ( $3N \times N-1$ ) array are zero.\* For each zero in  $S$ , place a ( $3 \times 1$ ) null vector at the corresponding position in the upper left ( $3N \times N-1$ ) corner of  $C$ . Choose a right-hand convention for positive rotations about principal axes of each body (consistent with the definition of  $A$ ), and express each mass center-to-hinge vector in these principal co-ordinates. For each nonzero element of  $S$ , multiply the corresponding mass center-to-hinge vector by  $S_{ij}$  and enter this product in the corresponding location of  $C$ .
- $A_E$  ("AE") A vector ( $N \times 1$ ) defining the effective surface area of each body, assuming 100% reflectivity for solar radiation pressure.
- $N_c$  ("NC") The total number of locked hinge axes in the system. (To clarify this definition it is noted that the system has  $3N-N_c$  rotational degrees of freedom). The present program capacity allows up to thirty-eight locked modes.
- $\mathcal{M}$  ("MI") A vector  $\{3(N-1) \times 1\}$  defined simply as follows: For every locked hinge axis identify the joint number ( $J$ ) and the locked mode ( $\alpha = 1, 2, 3$  for  $x, y, z$  respectively); compute the argument  $j = 3(J-1) + \alpha$ . Number the locked modes  $1, 2, \dots, N_c$  and, for each value of ( $j$ ) representing a locked mode, set  $M_j$  equal to this index number. For all other values of ( $j$ ), set  $M_j$  to zero.

---

\*These locations are used at a later point, after  $C$  is no longer needed and its storage is utilized for other purposes.

$J'_E$  ("XJE") Thermal bending constant computed as shown in Equation (A-19) from Earth heat flux ( $J_E$ ; Equation A-15); linear thermal coefficient of expansion ( $e$ ); boom segment length ( $l$ ), diameter ( $d$ ), thickness ( $\delta$ ), earth heat absorptivity ( $a_E$ ), and thermal conductivity ( $K$ ).

$J'_S$  ("XJS") Thermal bending constant computed as shown in Equation (A-19) from the above parameters, with ( $J_E$ ) and ( $a_E$ ) replaced by the solar heat flux ( $J_S$ ; Equations A-16 and A-17) and solar heat absorptivity ( $a_S$ ), respectively.

### Initial Conditions and Program Control

- $\Theta$  ("TH") A third order tensor ( $N \times 3 \times 3$ ) containing the direction cosine transformation from each set of body axes (defined for C above) to reference axes.\* The reference axes are defined by the upward local vertical (+Z) and the orbit pole (+Y).
- $\omega$  ("WV"; "WM") A vector ("WV";  $3N \times 1$ ) equivalenced to a matrix ("WM";  $3 \times N$ ) containing the absolute angular rate for each body, expressed in its own (principal axis) co-ordinate frame.\*
- $T$  ("ORBS") Total number of orbits to be simulated in one run.
- $N_R$  ("ENR") Number of readouts per orbit.
- $E_L$  ("ERL") A vector ( $12N \times 1$ ) of allowable absolute error per integration step for angular rates (rad./sec.; 1 to  $3N$ ) and direction cosines ( $3N + 1$  to  $12N$ ).

\*It is thus seen that these addresses contain the desired information (satellite attitude, shape, angular rates) which can be read out at any time. To begin the computer run, the initial values are stored in these locations.

### Astronomical Parameters

$a_0$ ("AZ")	Semi-major axis of orbit.
$e_0$ ("EZ")	Eccentricity of orbit. (The present program assumes $e_0 \leq 0.1$ , but an extension could readily be made).
$t_0$ ("TZ")	Time at periapsis, relative to the time ( $t = 0$ ) at the start of the simulation run.
$i_0$ ("EYZ")	Orbital inclination.
$\Omega_0$ ("THZ")	Longitude of the ascending node.
$\omega_0$ ("WZ")	Argument of the perigee.
$N_D$ ("ND")	Launch date (e.g., $N_D = 1$ for January 1).

For most programs it will be convenient to compute many of the above parameters from other, more basic, inputs (e.g., length, modulus of elasticity, angles at connecting points, etc.). This portion of the program will therefore consist of (a) Part I; controllable (punched card) inputs, and (b) Part II; fixed and derived inputs. Again, reference is made to Appendix B for an illustration. It is noted that the present program setup calls for inputs in MKS units, and the above angle inputs should be expressed in degrees. Also, any of the above provisions (auxiliary variables, additional dimension statements, print-out directions, etc.) must also be added to suit the individual problem under consideration. In general, the desired readouts will be simple functions of the angular rates ( $\omega$ -array) and attitude matrices ( $\theta$ -array).

## GENERAL PROGRAM COMPUTATIONS

The preceding introductory material contains the information required for program utilization. For those interested in the approach, the present discussion describes the fundamentals of the formulation (Refs. 1-3), and additional detail is included in the Appendix.\*

To determine the behavior of coupled rigid body motion, the rotational dynamics are first expressed as a set of equations in the usual form,

$$[I] \dot{\underline{\omega}} + [\tilde{\omega}][I]\underline{\omega} = \underline{\mathcal{T}} \quad (1)$$

where  $[I]$ ,  $\underline{\omega}$ ,  $[\tilde{\omega}]$ , and  $\underline{\mathcal{T}}$  denote inertia tensor, angular rate vector, the operator ( $\underline{\omega} \times$ ), and total torque vector, respectively. Since this Euler relation holds for each of the (N) members of the structure, Eq. (1) can be thought of as a (3N) dimensional equation;  $\underline{\omega}$  therefore has (3N) components, representing the absolute angular rate of each member as previously defined. The total torque vector  $\underline{\mathcal{T}}$  consists of (a) external torques, (b) internal torques, and (c) moments of internal forces. Since the internal forces are generally unknown and are not of primary interest in themselves, it is desirable to replace them by equivalent quantities obtained from Newton's laws. Consequently the internal forces are re-expressed in terms of external and d'Alembert forces; the motion of the composite structure mass center is then eliminated from the equations. As a result, the d'Alembert forces can be defined by second derivatives of position vectors relative to this composite mass center. Through the dynamical formalism, the moments of these d'Alembert forces are written in a convenient computational arrangement whereby

\*This report describes only the details of implementing the dynamic computations; for details of the formalism itself the reader is referred to Ref. 3.



- (1) part of the centripetal component is included as a constituent  $\underline{Q}$  of the total torque  $\underline{\mathcal{T}}$  ;
- (2) the remainder of the centripetal component is taken into account through replacing  $[\underline{I}]$  in the second term of Eq. (1) by a constant augmented inertia matrix  $[\underline{K}]$  ;
- (3) the tangential component (associated with  $\dot{\underline{\omega}}$  ) is taken into account through replacing  $[\underline{I}]$  in the first term of Eq. (1) by the augmented inertia matrix  $[\underline{K} + \underline{\Psi}]$  , where  $[\underline{\Psi}]$  varies as a known function of the previously defined attitudes  $[\underline{\theta}]$  .

With the external and internal torques, and the moments of the external forces denoted (as in Ref. 3) by  $\underline{L}$  ,  $e^T \circ [\underline{S}] \underline{\mathcal{Z}}$  , and  $[\underline{P}] \underline{F}$  respectively, Eq. (1) is rewritten as Eq. (15) of Ref. 3:

$$[\underline{K} + \underline{\Psi}] \dot{\underline{\omega}} + [\underline{\tilde{\omega}}][\underline{K}] \underline{\omega} = \underline{L} - [\underline{P}] \underline{F} + e^T \circ [\underline{S}] \underline{\mathcal{Z}} + \underline{Q} \quad (2)$$

To adapt this formulation to the present program, the two terms in the gravity gradient expression (Eq. 19 of Ref. 3) are symbolized here as  $(\underline{H} - \underline{G}')$  respectively; the transformed force vector  $\underline{G}''$  is then substituted for  $\underline{G}'$  to include solar pressure effects (Eqs. A-40 and A-41 in Appendix A of this report). The first two terms on the right of Eq. (2) can then be expressed as

$$\underline{L} - [\underline{P}] \underline{F} = \underline{H} - \underline{G}'' \quad (3)$$

The internal torque vector is then separated into two constituents as suggested in Ref. 2;

$$e^T \circ [\underline{S}] \underline{\mathcal{Z}} = \underline{\mathcal{Z}}' + [\underline{F}] \underline{T}_c \quad (4)$$

where  $\underline{\mathcal{Z}}'$  includes all spring and damper torques while  $\underline{T}_c$  is a vector in which the ( $i^{\text{th}}$ ) component represents the constraint torque in the ( $i^{\text{th}}$ ) locked mode (see the definitions for  $N_c$  and  $\mathcal{M}$  in the preceding section);  $[\mathcal{F}]$  is the matrix defined by Eq. (A-28). The quantities on the left of Eq. (2) are written as

$$[\Gamma] \triangleq [K + \Psi] \quad ; \quad \underline{W} \triangleq [\tilde{\omega}][K]\underline{\omega} \quad (5)$$

so that

$$[\Gamma] \underline{\dot{\omega}} = \underline{E} + [\mathcal{F}]\underline{T}_c \quad (6)$$

where

$$\underline{E} = -\underline{W} + \underline{H} - \underline{G}'' + \underline{\mathcal{Z}}' + \underline{Q} \quad (7)$$

In Appendix A it is shown that this leads to an expression of the form

$$[\Gamma] \underline{\dot{\omega}} = \underline{E} - [\mathcal{F}] \left\{ [\mathcal{F}]^T [\Gamma]^{-1} [\mathcal{F}] \right\}^{-1} \left\{ [\mathcal{F}]^T [\Gamma]^{-1} \underline{E} + \underline{\nu} \right\} \quad (\text{A-31})$$

which is the actual equation solved through numerical integration in this program.

Just as the specific system portion of the program has been divided into (a) Part I - Controlled inputs, (b) Part II - Fixed and derived inputs, and (c) Readouts, the general program operations fall into three categories:

- (a) Part 0 - Program setup (e.g., dimensions, physical constants, etc.)
- (b) Part III - General system constants (e.g., barycentric vectors as defined in Ref. 3, etc.), and
- (c) Part IV - Evaluation of derivatives and numerical integration.

The Fortran nomenclature and operation sequence were chosen to maintain reasonable storage requirements without incurring any appreciable loss in computation efficiency. The six largest arrays consume roughly twenty thousand storage locations,

accommodating a maximum of 26 members and up to 38 locked modes for the complete satellite assembly. All steps of the general computation are identified in Appendix C.

## APPENDIX

Most of the detailed theoretical background for the gravity gradient satellite program is contained in Ref. 3. In restricting the Roberson-Wittenburg approach to this application, however, it was found that additional aspects of the formulation (e.g., hinge moments, additional forces, etc.) could be defined more specifically with little further loss of generality. The various computations added to the general program are described in Appendix A.

In order to illustrate in a concrete manner how this program can be applied to an existing satellite, a model of the Radio Astronomy Explorer<sup>4</sup> is described in Appendix B. A detailed description of the computation then follows in Appendix C, in the form of an annotated Fortran listing.

It was found convenient to treat much of the notation in an individual sectional basis, with various quantities defined in the text of the derivations. The Roberson-Wittenburg notation<sup>3</sup>, however, and its additions (e.g., augmentation of external force by the solar pressure, etc.) described in the body of this report, are retained. Components of torques, angular rates, and angular accelerations, for example are expressed in the co-ordinate frame of the appropriate structural member; it follows that vector equations are generally written in these body co-ordinates. The IJK index (previously defined in terms of the incidence matrix  $[S]$  and the satellite shape  $[L]$ ), and much of the additional notation defined in the body of the report, arises repeatedly throughout the analysis. For the model of gravity gradient booms, the cross-section is presumably circular (either solid or hollow); the length is chosen along the body x-axis, with (y) and (z) along the principal inertia axes of the cross-section. In all cases, the principal inertia axes are used for body co-ordinates, and standard right hand conventions are used for angle transformations; the matrix notations  $[ ]^T$ ;  $tr[ ]$ ; and

$[\rho]_{\mu}$  represent transpose; trace; and an orthogonal transformation obtained by a positive rotation of  $(\beta)$  radians about the u-axis, respectively.  $\frac{1}{\alpha}$  represents the  $(\alpha)$  column of the  $3 \times 3$  identity matrix  $[I_{33}]$ .

APPENDIX A  
ANALYTICAL FORMULATIONS APPLICABLE TO  
THE GENERAL PROGRAM

In Ref. 3 the hinge moment computation was left open in order to maintain generality of scope for the dynamical formalism. For the gravity gradient satellite program it has been found that the torque at each joint can be characterized by a convenient formulation applicable to numerous hinge types. The method uses straightforward program logic based on the incidence matrix  $[S]$ , with the torque computed from the eigenvector and trace angle of the orthogonal transformation between adjacent members. When the "rest position" of one member relative to another is variable (e.g., due to thermal bending), the same basic formulation is augmented in a straightforward manner. The "locked mode" torque described in Ref. 2, for hinges with less than three degrees of freedom, has also been programmed.

In addition to providing explicit hinge moment computations, the program includes the force on each member due to solar radiation pressure. Finally there is a kinematical relation appropriate for satellites in low eccentricity orbits, and the position of the sun must also be defined in relation to satellite orientation. All of these items are covered by the analytical background material in this Appendix.

Hinge Torques

From the INTRODUCTION it is recalled that the undeformed shape of the satellite is defined in terms of the matrices  $[P_J]$ , where  $J (\leq N-1)$  is the hinge index number. The next section illustrates how a modified matrix  $[P'_J]$  performs this function when thermal effects are included. It follows that the reaction torque at hinge  $J$  is zero when the relative orientation  $\{[V']\}$

$\hat{= } \{ [\mathbf{e}_i]^T [\mathbf{e}_k] \}$  of the two members touching this hinge is equal to  $[\rho_j']$  ;  
 in general the hinge moment is a function of the deformation matrix,

$$[\mathbf{V}] = [\rho_j'] [\mathbf{V}']^T \quad (\text{A-1})$$

More specifically, the reaction torque is a function of the trace angle,

$$\lambda = \text{Arccos} \left\{ \frac{1}{2} \text{tr} [\mathbf{V}] - \frac{1}{2} \right\} \quad (\text{A-2})$$

and the unit eigenvector  $\underline{\mathbf{U}}$  of  $[\mathbf{V}]$  which points along the positive axis of rotation. This vector satisfies the equation (denoting the 3 x 3 identity by I),

$$[\mathbf{V} - \mathbf{I}] \underline{\mathbf{U}} = \underline{\mathbf{0}} \quad (\text{A-3})$$

and therefore can be computed from the cross product of any two nonvanishing\* rows of  $[\mathbf{V} - \mathbf{I}]$  .

The product  $(\lambda \underline{\mathbf{U}})$  can be thought of as a displacement vector which generates a reaction torque. Immediately this suggests the form for the "position feedback" torque for a linear system having negligible delay:  $\lambda [\mathbf{R}_j] \underline{\mathbf{U}}$  , where  $[\mathbf{R}_j]$  is the restraining matrix for hinge  $\mathbf{J}$  , described in Section 1.1. For attitude control problems the elements of  $[\mathbf{R}]$  are easily identified as the controller sensitivities; for structural applications  $[\mathbf{R}]$  consists of rigidity coefficients which are readily derived from the small angle\*\* flexure and torsion formulas,

\*e.g., when  $\underline{\mathbf{U}}$  is along the x-axis the first row of  $[\mathbf{V} - \mathbf{I}]$  will vanish. Furthermore, when  $\underline{\mathbf{U}}$  is too close to the x-axis the use of the first row of  $[\mathbf{V} - \mathbf{I}]$  in the computation would lead to numerical problems. Program logic avoids inaccuracy of this type.

\*\*This restriction of course holds only for structural reaction torques. In contrast to restricting the scope of application, moreover, this can be viewed as a requirement imposed upon (N) since the angles can be made smaller by separating the model into a larger number of segments. Finally, it is noted that the hinge moment formulation could be modified to account for larger angles.

$$\text{Bending Moment} \doteq E \mathcal{J} \frac{d\theta_B}{dl} \quad (\text{A-4})$$

$$\text{Torsion Moment} = G \mathcal{J} \frac{d\theta_T}{dl} \quad (\text{A-5})$$

where  $E$ ,  $G$ ,  $\mathcal{J}$ , and  $\mathcal{J}$  represent Young's modulus and the shear modulus of elasticity, the in-plane and polar area inertia moments of the structural member cross-section, respectively;  $(d\theta_B/dl)$  is a measure of bending curvature which can be approximated\* by  $(\lambda U_i/l)$ , where  $U_i$  is the component of  $\underline{U}$  along the axis implied in Equation (A-4), and  $(l)$  is the distance between centers of the members joined by hinge  $\mathcal{J}$ ; a similar approximation is used for the torsional gradient  $(d\theta_T/dl)$ . It follows that, for structural members with no inherent coupling between bending and torsion (such as that which would arise from displacement between mass and shear centers),  $[R_J]$  is a diagonal matrix with elements  $(G \mathcal{J}/l)$ ,  $(E \mathcal{J}_y/l)$ , and  $(E \mathcal{J}_z/l)$ , where  $\mathcal{J}_y$  and  $\mathcal{J}_z$  correspond to principal axes of the cross-section.\*

In addition to the above position feedback or elastic reaction, there may be a moment restraining relative angular rate between adjacent members. From the definition of  $[R']$  it follows that this component of torque in the coordinates of body  $I$  is

$$[R'_J](\underline{\omega}'_K - \underline{\omega}'_I) ; \quad \underline{\omega}'_K \triangleq [V'] \underline{\omega}_K \quad (\text{A-6})$$

and (recalling from Section 1.1 that  $[R]$  and  $[R']$  are referenced to body  $I$ ) the total hinge moment acting on body  $I$  is

$$\underline{\alpha}'_I = \lambda [R_J] \underline{U} + [R'_J](\underline{\omega}'_K - \underline{\omega}'_I) \quad (\text{A-7})$$

\*In many applications this first approximation will be inadequate; Appendix B illustrates a refined approximation method for  $(d\theta_B/dl)$  which was successfully applied to the RAE program.



and the hinge moment on body K is

$$\underline{z}'_K = -[v']^T \underline{z}'_I \quad (A-8)$$

This completes the discussion for this portion of the program. Before leaving this topic it is noted that ( 1 ) various nonlinear functions of the deformation (  $\lambda \underline{U}$  ) and/or the relative rate (  $\underline{\omega}'_K - \underline{\omega}'_I$  ) could easily be programmed, to simulate nonlinear reaction torque characteristics encountered in practice; and ( 2 ) delayed feedback torque supplied from band-limited devices could be computed by standard convolution integral techniques.

### Thermal Bending

Gravity gradient satellites often employ long narrow booms which are prone to nonuniform heating. A convenient way to take this into account is to replace the zero torque rest position matrix  $[\rho_J]$  for each hinge by a new matrix  $[\rho'_J]$  which defines the reference shape under uneven heating conditions. This new matrix can be formed by a simple orthogonal transformation of its original value,

$$[\rho'_J] = [-\delta_z]_z [+ \delta_y]_y [\rho_J] \quad (A-9)$$

where the bending angles (  $\delta_y$  ) and (  $\delta_z$  ) are identified by combining this expression with equation (A-1):

$$[v] = [-\delta_z]_z [+ \delta_y]_y [\rho_J] [v']^T$$

Structural deformation is zero when  $[v]$  is the identity matrix. Since  $[v']^T$  is the transformation from actual I to K co-ordinates and  $[\rho_J]$  is the transformation from K to original reference axes of I, it follows that the product  $[-\delta_z]_z [+ \delta_y]_y$  must be the transformation from the original (undeformed) to the new rest position (zero torque) axes of body I. This angular displacement of

the reference orientation for each segment in the discrete model is obtained by inscribing a set of chords ( $n =$  number of segments per boom) inside the arc formed by thermal bending. The present description will begin with an example of planar bending caused by a single heat source, followed by extension to the general case.

In Fig. 1,  $J$  denotes the hinge connecting body I (represented by the chord  $JJ'$ ) to body K, which may be visualized on the left of the hinge.

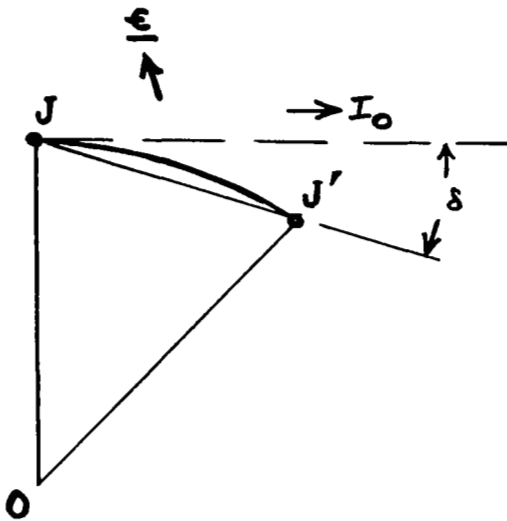


Fig. 1 Effect of Thermal Bending

The reference orientation of the I segment in the absence of heating effects will be taken along the direction of the arrow  $I_0$ . Thus  $\delta$  is the bending angle due to a heat source in the direction  $\underline{\epsilon}$ , tentatively defined in the plane of the figure.

Under the above conditions the arc  $JJ'$  is essentially circular\* with center at O and radius of curvature  $R_c$  meters. With ( $l$ ) again defined as the distance between centers of the members joined by hinge  $J$ , it is seen

that the average change in angle per unit length is ( $\delta/l = 1/R_c$ ) and, combined with Eq. (4) of Ref. 5,

$$\delta = \frac{e l}{d} (\Delta T) \tag{A-10}$$

\*Just as in the preceding section, this small angle approximation is valid provided that the model contains a sufficient number of segments.

where  $e$ ,  $d$ , and  $(\Delta T)$  denote the linear thermal coefficient of expansion  $(^{\circ}\text{C})^{-1}$ , boom diameter (meters), and diametric temperature differential ( $^{\circ}\text{C}$ ), respectively. With the unit vector along the segment  $\approx$  (length) axis  $\underline{JJ}'$  denoted by  $\underline{1}_1$ , it is seen that a direction\* for  $\underline{\delta}$  can be defined by the unit vector  $\left\{ \underline{\epsilon} \times \underline{1}_1, / |\underline{\epsilon} \times \underline{1}_1| \right\}$ . By reason of the small angle approximation for adjacent segments, then, the finite rotation can be treated as a vector,

$$\underline{\delta} = \frac{e l}{d} (\Delta T) \frac{\underline{\epsilon} \times \underline{1}_1}{|\underline{\epsilon} \times \underline{1}_1|} \quad (\text{A-11})$$

Since  $|\underline{\epsilon} \times \underline{1}_1|$  is equivalent to the cosine of the angle between  $\underline{\epsilon}$  and the normal to the segment, Eq. (6) of Ref. 5 can be written here as

$$\frac{\Delta T}{|\underline{\epsilon} \times \underline{1}_1|} = \frac{d^2}{4 K \mathcal{F}} (a q) \quad (\text{A-12})$$

and, therefore,

$$\underline{\delta} = \frac{e l d}{4 K \mathcal{F}} (a q) (\underline{\epsilon} \times \underline{1}_1) \quad (\text{A-13})$$

in which  $K$ ,  $\mathcal{F}$ ,  $a$ , and  $q$  represents thermal conductivity (large calories/second-meter- $^{\circ}\text{C}$ ), boom thickness (meters), and the absorptivity and heat radiation (large calories/second-meter<sup>2</sup>) of the source, respectively. The convenience of this formulation is apparent when different heat sources are combined; with direct earth radiation and direct plus reflected solar radiation (at an albedo<sup>6</sup> of 0.4), the unit vectors in the source directions are denoted as

\*The cross product conforms to the definition of  $[\underline{\delta}]$  as the transformation from the original to the deformed rest position of segment I.

$$\underline{\epsilon}_{\text{Solar}} = \begin{bmatrix} \sigma_{I1} \\ \sigma_{I2} \\ \sigma_{I3} \end{bmatrix} ; \quad \underline{\epsilon}_{\text{Earth}} = \begin{bmatrix} -\theta_{I31} \\ -\theta_{I32} \\ -\theta_{I33} \end{bmatrix}$$

and the thermal deflection angles are computed from resultants thus: For the y-axis, the right of Eq. (A-13) is written with the substitutions,

I. Direct Earth

- 1)  $a = a_E$ , absorptivity for earth radiation.
- 2)  $\mathcal{F} = \mathcal{F} J_E$ , where  $\mathcal{F}$  is computed from the earth radius ( $R_E$ ) and the Keplerian orbital distance ( $r$ ) as<sup>7</sup>

$$\mathcal{F} = 2 \left[ 1 - \sqrt{1 - (R_E/r)^2} \right] \quad (\text{A-14})$$

and  $J_E$  is the Stefan-Boltzmann constant ( $5.67 \times 10^{-8}/4184$  large calories per sec per sq. meter per  $^{\circ}\text{K}^4$ ) multiplied by the fourth power of the effective<sup>8</sup> spherical blackbody Earth temperature ( $246^{\circ}\text{K}$ ):

$$J_E = \frac{5.67 \times 10^{-8}}{4184} (246)^4 \quad (\text{A-15})$$

$$3) \quad [\underline{\epsilon} \times \underline{1}_1] \cdot \underline{1}_2 = -\theta_{I33}$$

II. Direct Solar

- 1)  $a = a_S$ , absorptivity for solar radiation.
- 2)  $\mathcal{F} = J_S (I_S - 1)$ , where

$$I_S = \begin{cases} 2, & \text{sun not eclipsed} \\ 1, & \text{sun eclipsed} \end{cases}$$

and  $J_S$  is the product

$$J_S = P_S c / 4184 \quad (A-16)$$

with  $c$  defined as the speed of light

( $3 \times 10^8$  m/sec) and

$$P_S = 4.5 \times 10^{-6} \text{ (Newt./m}^2\text{)} \quad (A-17)$$

$$3) \quad [\underline{\epsilon} \times \underline{1}_1] \cdot \underline{1}_2 = \sigma_{I3}$$

### III. Reflected Solar

$$1) \quad a = a_s$$

2)  $\mathcal{F} = .4 \mathcal{F} J_S (I_S - 1)$ , where all of these quantities are defined above. It is noted that  $\mathcal{F}$  is not the true coefficient to be used for reflected radiation, but it provides an excellent approximation.<sup>7</sup>

$$3) \quad [\underline{\epsilon} \times \underline{1}_1] \cdot \underline{1}_2 = -\theta_{I33}$$

The total rotation about the y-axis due to thermal bending is therefore

$$\delta_y = -\mathcal{F} J'_E \theta_{I33} + J'_S (\sigma_{I3} - .4 \mathcal{F} \theta_{I33}) (I_S - 1) \quad (A-18)$$

where

$$J'_E = \frac{e l d a_E}{4 K \mathcal{F}} J_E ; \quad J'_S = \frac{e l d a_S}{4 K \mathcal{F}} J_S \quad (A-19)$$

and, similarly, thermal bending about the z-axis is obtained by the negative

$\{[\underline{\epsilon} \times \underline{1}_1] \cdot \underline{1}_3 = -\epsilon_2\}$  angle transformation in Eq. (A-9) with

$$\delta_z = -\mathcal{F} J'_E \theta_{I32} + J'_S (\sigma_{I2} - .4 \mathcal{F} \theta_{I32}) (I_S - 1) \quad (A-20)$$

Thermal bending throughout the entire structure is accounted for by repeating these computations at every applicable hinge. For example, in the case of a nominally straight boom, the reference direction for the segment to the right of  $J'$  is the extended line  $JJ'$ ; this segment is then denoted as I in computing the bending angles at  $J'$ , while the chord  $JJ'$  takes the role of segment K. The preceding formulation then applies to the computation of angles at  $J'$ , and likewise to all hinges where thermal bending can occur.

As a further refinement it is noted that the matrix  $[-\delta_z]_z[+\delta_y]_y$  can be replaced by

$$[\delta] = \begin{bmatrix} \tau & -\delta_z & -\delta_y \\ \delta_z & \frac{\delta_y^2 + \tau\delta_z^2}{\delta_y^2 + \delta_z^2} & \frac{\delta_y\delta_z(\tau-1)}{\delta_y^2 + \delta_z^2} \\ \delta_y & \frac{\delta_y\delta_z(\tau-1)}{\delta_y^2 + \delta_z^2} & \frac{\delta_z^2 + \tau\delta_y^2}{\delta_y^2 + \delta_z^2} \end{bmatrix}; \tau \triangleq \sqrt{1 - \delta_y^2 - \delta_z^2} \quad (A-21)$$

It has been verified that this matrix is orthogonal and that the x-component of its real eigenvector is zero.

#### Constraint Torques at Locked Joints

In many instances there are hinges which are constructed to allow only one or two degrees of freedom, or it may be desirable to remove a degree of freedom from the computation model.\* When a hinge constrains relative motion about the  $\alpha$ -axis ( $\alpha = 1, 2, 3$  for  $x, y, z$  respectively) of a given member (I) of the structure, the  $\alpha$ -component of the relative angular rate between body I and K, expressed in I-coordinates, is set to zero:

\*e.g., if the torsional natural frequencies of a gravity gradient boom are very high, it may be convenient to assume that only flexure is possible.

$$\underline{\mathbf{1}}_{\alpha}^T \{ \underline{\omega}_I - [\theta_I]^T [\theta_K] \underline{\omega}_K \} = 0 \quad (\text{A-22})$$

As noted in Ref. 2, the first step in deriving the constraint torque is to differentiate the above expression. It is shown in a later section of this Appendix that

$$d/dt [\theta_I] = [\theta_I] [\Omega_I] - [N] [\theta_I] \quad (\text{A-23})$$

(where  $[\Omega]$  and  $[N]$  are skew-symmetric angular rate matrices), so that

$$\underline{\mathbf{1}}_{\alpha}^T \dot{\underline{\omega}}_I - \underline{\mathbf{1}}_{\alpha}^T \{ ([\Omega_I]^T [\theta_I]^T - [\theta_I]^T [N]^T) [\theta_K] \underline{\omega}_K + [\theta_I]^T ([\theta_K] [\Omega_K] - [N] [\theta_K]) \underline{\omega}_K + [\theta_I]^T [\theta_K] \dot{\underline{\omega}}_K \} = 0 \quad (\text{A-24})$$

This is simplified by accounting for 1) the skew-symmetric character of  $[\Omega]$  and  $[N]$ , and 2) the property  $[\Omega_K] \underline{\omega}_K = \underline{\mathbf{0}}$ ; introducing the previously defined notations  $[V']$  and  $\underline{\omega}'_K$ ,

$$\underline{\mathbf{1}}_{\alpha}^T \{ \dot{\underline{\omega}}_I - [V'] \dot{\underline{\omega}}_K \} = -\underline{\mathbf{1}}_{\alpha}^T [\Omega_I] \underline{\omega}'_K \quad (\text{A-25})$$

There will be a scalar equation of this form for every combination  $(J, \alpha)$  which represents a locked joint constraint. It is therefore appropriate to define an identifying argument  $(j)$  for each locked mode,

$$j = 3(J - 1) + \alpha \quad (\text{A-26})$$

plus a column vector  $\underline{m}$  having  $3(N-1)$  components such that  $m_j$  is zero for all unlocked modes and, for locked modes,  $m_j$  is an integer representing the ordered index of that mode ( $1 \leq m_j \leq N_c$ , where  $N_c$  is the total number

of locked modes). The set of equations (A-25) can then be written in matrix form

$$[\mathcal{F}]^T \underline{\dot{\omega}} = -\underline{\nu} \quad (\text{A-27})$$

where  $[\mathcal{F}]$  is a  $(3N \times N_c)$  matrix in which the only nonzero elements are the unit vector components

$$\underline{f}_{I, m_j} = \underline{1}_\alpha^T ; \quad \underline{f}_{K, m_j} = -\underline{1}_\alpha^T [V'] \quad (\text{A-28})$$

in the  $m_j$  row and the  $I^{\text{th}}$  and  $K^{\text{th}}$  triplet of columns respectively,  $I$  and  $K$  representing the bodies constrained by the  $m_j$  locked mode. The vector  $\underline{\dot{\omega}}$  in (A-27) is the same angular acceleration vector appearing in the Roberson-Wittenburg equation; and  $\underline{\nu}$  is a vector  $(N_c \times 1)$  whose  $m_j$  component is

$$\nu_{m_j} = \underline{1}_\alpha^T [\Omega_I] \underline{\omega}'_K \quad (\text{A-29})$$

where  $(\alpha, I, K)$  of course correspond to the locked mode under consideration.

At this point, Eq. (6) is premultiplied by  $[\mathcal{F}]^T [\Gamma]^{-1}$  and combined with (A-27):

$$\underline{T}_c = -\{[\mathcal{F}]^T [\Gamma]^{-1} [\mathcal{F}]\}^{-1} \{[\mathcal{F}]^T [\Gamma]^{-1} \underline{E} + \underline{\nu}\} \quad (\text{A-30})$$

so that the final differential equation is

$$[\Gamma] \underline{\dot{\omega}} = \underline{E} - [\mathcal{F}] \{[\mathcal{F}]^T [\Gamma]^{-1} [\mathcal{F}]\}^{-1} \{[\mathcal{F}]^T [\Gamma]^{-1} \underline{E} + \underline{\nu}\} \quad (\text{A-31})$$



## Radiation Pressure

The present formulation involves the effective solar radiation force on each member of the structure, expressed in the co-ordinates of that member. Although the pertinent theory is well-known, an example of a typical boom segment (again denoted here as "body I") is treated here to illustrate application to the problem at hand.

It is convenient to begin by considering a flat surface of area  $A$  subjected to a radiation pressure from a source along the unit sunline vector  $\underline{\sigma}_I$  (see Eqs. A-50 — A-54). With the force per unit area of  $A$  denoted by  $(\phi)$ , the component of the effective force along  $\underline{n}_A$  due to incident radiation has a magnitude  $\phi A |\underline{\sigma}_I \cdot \underline{n}_A|$ , where  $\underline{n}_A$  is the unit normal to the surface  $A$ . With perfect reflection, the total force due to incident plus reflected radiation is directed along  $(-\underline{n}_A)$  and has a magnitude

$$|F_A| = 2\phi A |\underline{\sigma}_I \cdot \underline{n}_A| \quad (A-32)$$

While  $(\phi)$  is defined as the force per unit area of  $A$ , it is more convenient to work with the characteristics of the source itself; it is easily shown that

$$\phi = P_S |\underline{\sigma}_I \cdot \underline{n}_A| \quad (A-33)$$

where  $P_S$  is defined by Eq. (A-18). It follows that

$$|F_A| = 2P_S (\underline{\sigma}_I \cdot \underline{n}_A)^2 A \quad (A-34)$$

Application of this theory to nonplanar surfaces is straightforward in principle and, for regular geometry, often leads to simple solutions. Each

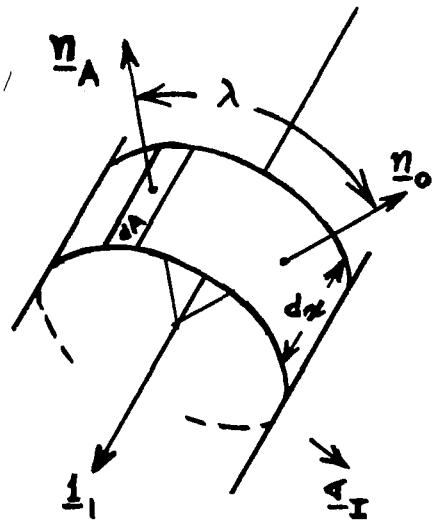


Fig. 2 Radiation Pressure on Section of Cylinder

section of a gravity gradient boom, for example, can be represented by a cylinder, centered about the boom torsion axis  $\underline{1}_1$ . Fig. 2 shows a small section of width ( $d\alpha$ ) with a principal normal (defined as the normal to the surface extending outward from the center of  $d\alpha$ , and lying in the plane of  $\underline{1}_1$  and  $\underline{\varphi}_I$ ) along the direction  $\underline{n}_o$ . It is permissible to consider the unit sunline vector  $\underline{\varphi}_I$  as originating from the intersection point of  $\underline{1}_1$ ,  $\underline{n}_o$ , and  $\underline{n}_A$ , so that the spherical law of cosines can be invoked:

$$(\underline{\varphi}_I \cdot \underline{n}_A) = (\underline{\varphi}_I \cdot \underline{n}_o) \cos \lambda \quad (\text{A-35})$$

where the significance of  $\underline{n}_A$  of course lies in its orthogonality to the differential surface area

$$dA = \frac{d}{2} d\lambda d\alpha \quad (\text{A-36})$$

in which ( $d$ ) represents boom diameter. Preparations are now complete for integrating the force over the cylindrical area. It is first noted that the component along  $\underline{1}_1$  vanishes in the present problem because the resultant must be normal to the surface; furthermore the component along  $(\underline{1}_1 \times \underline{n}_o)$  vanishes by symmetry. For the differential area  $dA$  the component of force along  $(-\underline{n}_o)$  is  $(dF_A \cos \lambda)$ ; it is this quantity which must be integrated using

(A-34) through (A-36):

$$F_{cyl} = 2P_S (\underline{\sigma}_I \cdot \underline{\eta}_0)^2 \left(\frac{d}{2}\right) \int_0^d \int_{-\pi/2}^{\pi/2} \cos^3 \lambda \, d\lambda \, dx \quad (A-37)$$

It can easily be shown that this is equivalent to  $2P_S A_E (\underline{\sigma}_I \cdot \underline{\eta}_0)^2$  where  $A_E$  is the cylindrical effective area,

$$A_E = \frac{2}{3} l d \quad (A-38)$$

Since the direction of the effective force is along the unit vector

$$-\underline{\eta}_0 = \frac{\underline{1}_1 \times (\underline{1}_1 \times \underline{\sigma}_I)}{|\underline{1}_1 \times (\underline{1}_1 \times \underline{\sigma}_I)|} = \frac{-1}{\sqrt{\sigma_{I2}^2 + \sigma_{I3}^2}} \begin{bmatrix} 0 \\ \sigma_{I2} \\ \sigma_{I3} \end{bmatrix} \quad (A-39)$$

the solar force vector expressed in I-co-ordinates is

$$\underline{F}_{cyl} = \begin{bmatrix} 0 \\ -\sigma_{I2} \\ -\sigma_{I3} \end{bmatrix} (2P_S) \sqrt{\sigma_{I2}^2 + \sigma_{I3}^2} A_E(I) \quad (A-40)$$

By a derivation along similar lines it can be shown that the effective radiation force vector for a sphere is

$$\underline{F}_{sph} = -\underline{\sigma}_I (2P_S) A_E(sph) \quad (A-41)$$

where the effective area for a sphere of radius ( $l_1$ ) is

$$A_E(sph) = \frac{1}{2} \pi l_1^2 \quad (A-42)$$

Presence of these forces must of course be subject to the condition of no eclipse.

### Kinematics

In this section the orthogonal matrices  $[B]$  ;  $[\theta_I]$  ; and  $[D]$  will denote transformations from principal axes of a structural member (body I) to a set of inertial axes; from the body axes to a set of local axes; and from the local to the inertial co-ordinates, respectively. It follows immediately that

$$[B] = [D][\theta_I] \quad (A-43)$$

and it is well-known that

$$d/dt [B] = [B][\Omega_I] \quad (A-44)$$

where  $[\Omega_I]$  is a skew-symmetric matrix of inertial angular rates ( $\Omega_{I,12} = -\omega_{I3}$ ;  $\Omega_{I,13} = +\omega_{I2}$ ;  $\Omega_{I,23} = -\omega_{I1}$ ). Defining the local axes by  $(+y)$  along the orbit pole and  $(+z)$  along the upward local vertical,

$$d/dt [D] = [D][N] \quad (A-45)$$

where  $[N]$  is a 3 x 3 matrix whose only nonzero elements appear in the positions ( $N_{13} = -N_{31}$ ) representing the time derivative of the true anomaly; from the appropriate equation on page 262 of Ref. 9 it can be deduced that

$$N_{13} = \sqrt{\mu_E p_0} / r^2 \quad (A-46)$$

where  $p_0 = a_0(1 - e_0^2)$ ;  $\mu_E$ ,  $r$ ,  $a_0$ , and  $e_0$  are defined as the Earth gravitational constant; the Keplerian orbit position vector magnitude, semimajor axis, and eccentricity, respectively.

By differentiation of (A-43),

$$d/dt [\theta_I] = [D]^T d/dt [B] + \{d/dt [D]\}^T [B] \quad (A-47)$$

and, in combination with (A-43) through (A-45),

$$\frac{d}{dt} [\theta_I] = [\theta_I] [\Omega_I] + [N]^T [\theta_I] \quad (A-48)$$

To compute the angular rate for the matrix  $[N]$  it is noted that gravity gradient satellites generally have low eccentricity (e.g., less than 0.1). The quantity ( $\lambda$ ) in (A-46) can therefore be determined explicitly by a series approximation on page 153 of Ref. 9; using the notation ( $A_m$ ) for the mean anomaly,

$$\lambda = a_0 \left[ 1 - e_0 \cos A_m - \frac{1}{2} e_0^2 (\cos 2A_m - 1) - \frac{1}{8} e_0^3 (3 \cos 3A_m - 3 \cos A_m) \right] \quad (A-49)$$

#### Astronomical Geometry

Solar position is determined using the celestial sphere model on page 9 of Ref. 9. A value of  $23.5^\circ$  is used as the ecliptic inclination and, on the ( $N_D$  <sup>th</sup>) day of the year, the sunline vector makes an angle of

$$\psi_s = 2\pi (N_D - 80) / 365 \quad (A-50)$$

with the vernal equinox. The sunline vector expressed in inertial (celestial sphere) co-ordinates is therefore

$$\underline{v}'' = \begin{bmatrix} \cos \psi_s \\ \cos 23.5^\circ \sin \psi_s \\ \sin 23.5^\circ \sin \psi_s \end{bmatrix} \quad (A-51)$$

To define this vector in local co-ordinates the inclination, longitude of the ascending node, and argument of the perigee for the satellite orbit are written as ( $i_0, \Omega_0, \omega_0$ ) respectively, and the true anomaly is computed explicitly by

the series approximation on page 154 of Ref. 9:

$$v = A_m + 2e_0 \sin A_m + \frac{5}{4} e_0^2 \sin 2A_m + \frac{1}{12} e_0^3 (13 \sin 3A_m - 3 \sin A_m) \quad (\text{A-52})$$

which is again accurate for most gravity gradient satellite applications ( $e_0 \leq 0.1$ ). The sunline in local co-ordinates is therefore

$$\underline{v}' = \begin{bmatrix} 0 & 1 & 0 \\ 0 & 0 & 1 \\ 1 & 0 & 0 \end{bmatrix} [\omega_0 + v]_{\underline{z}} [i_0]_x [\Omega_0]_{\underline{z}} \underline{v}'' \quad (\text{A-53})$$

The unit vector pointing toward the sun, expressed in body I-axes, is then obviously,

$$\underline{v}_I = [\theta_I]^T \underline{v}' \quad (\text{A-54})$$

and it is this vector which is used for the appropriate thermal bending and radiation pressure computations.

This completes the description of analytical formulations used in the gravity gradient satellite program. The next Appendix describes an example configuration (RAE satellite<sup>4</sup>).

## APPENDIX B

### THE RADIO ASTRONOMY EXPLORER (RAE) SATELLITE CONFIGURATION AND PARAMETERS

The RAE satellite described in Ref. 4 is cruciform shaped, passively damped with a horizontal libration damper boom skewed out of the plane of the cruciform.<sup>10</sup> The typical RAE example configuration is shown in Fig. 3 with the flexible antenna booms approximated dynamically with 3 rigid segments per boom. The four 750 foot antenna booms in their undeformed state make an angle of 30 degrees with the  $\underline{Z}_{HUB}$  axis in the cruciform plane. The damper boom (assumed rigid) is spring restrained to its reference position relative to the hub, and is skewed at an angle of 65 degrees from the cruciform plane. Each rigid body or member and each hinge is indexed as shown in figure 3. The hinge numbers are denoted by an underline. For a larger number of segments per boom, the same counter-clockwise numbering scheme would be used.

Each member has a body-fixed set of right-hand coordinates defined collinear with the principal inertia axes, and the origin is the mass center of each member. Only the direction of two axes need be given for the right hand coordinate frame to be well defined. The hub axes are shown in Fig. 3. THE FOLLOWING COORDINATE FRAMES OF THE REMAINING MEMBERS ARE DEFINED WITH THE SATELLITE IN ITS UNDEFORMED CONFIGURATION, and it should be remembered that the axes remain fixed in each member even after relative rotational displacement between them:

The damper boom  $\underline{Z}$  and  $\underline{X}$  axes are in the direction of  $\underline{Z}_{HUB}$  and the outward directed damper boom centroidal axis respectively. In each antenna boom segment the  $\underline{Y}$  and  $\underline{X}$  axes are in the direction of  $\underline{Y}_{HUB}$

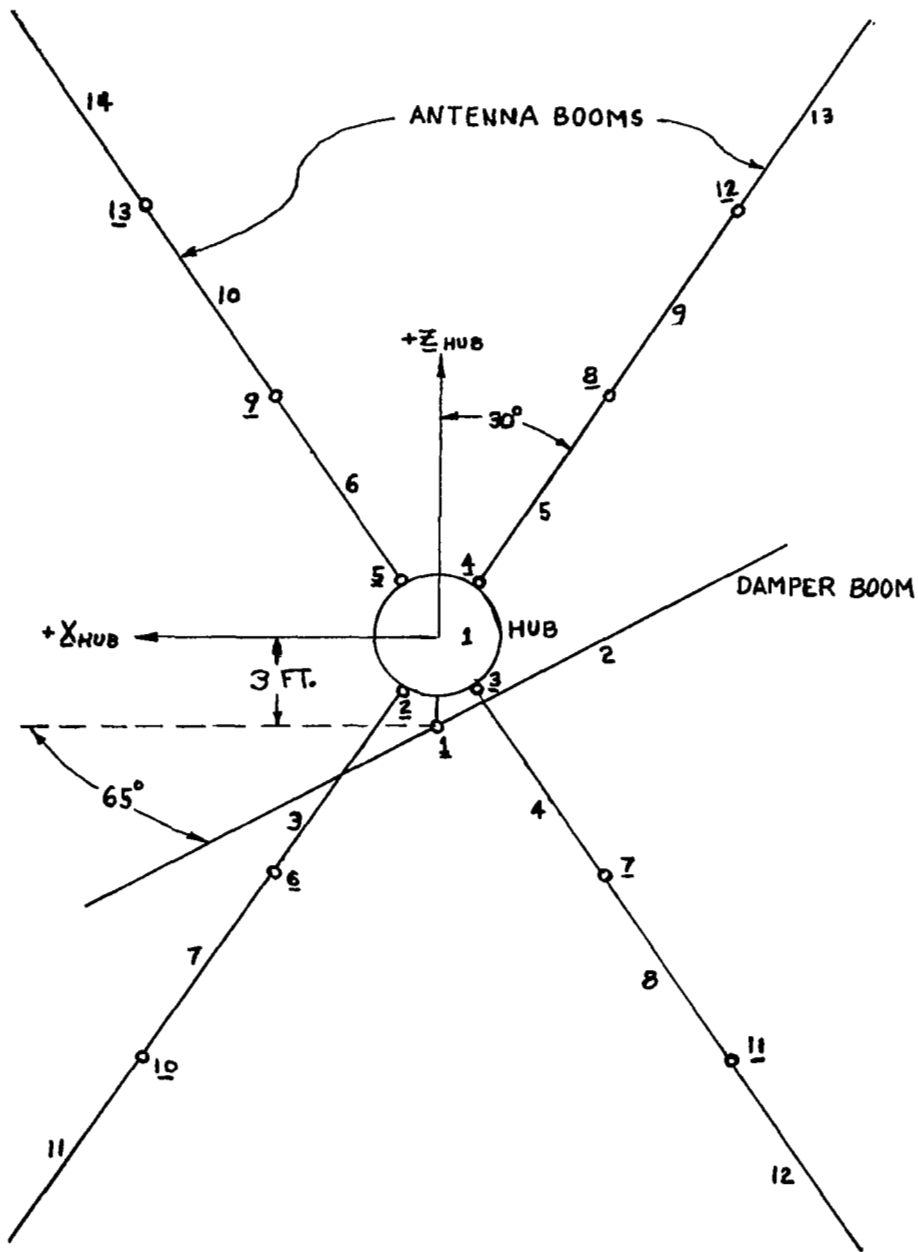


Fig. 3 RAE Configuration



and the outward directed antenna segment centroidal axis respectively. For radiation pressure effective area computations the hub is assumed spherical in shape, while the damper boom and all antenna segments are cylindrical. It is noted that the damper boom is free to rotate about its Y axis only.

All parameters in the RAE simulation are expressed in MKS units. However, since many RAE satellite properties are given in English units, appropriate conversion factors are listed below. Following this is a description of RAE variable inputs (Part I), fixed and derived inputs (Part II), and inputs to the general program (Parts III and IV) as defined in the INTRODUCTION of this report\*. Included also are the formulations for initial conditions, magnetic hysteresis damping torque, and readouts.

#### MKS Units

Length - Meters (m)

Mass - Kilograms (Kg)

Temperature - Degrees Centigrade (°C)

Heat - Large Calories (K-cal; i.e., the amount of heat required to raise the temperature of 1 KG-H<sub>2</sub>O by 1°C.)

Force - Newtons (Newt)

#### Conversion Factors

.3048m = 1 ft.

14.5939 Kg = 1 slug

1 Newt = .2248 lbs.

4184 Kcal = 1 Newt-m = 1 Joule

---

\*Along with the mathematical symbol, the actual Fortran statement as used in the program is given in quotation.

RAE VARIABLE INPUTS (PART I)

System Parameters

$n$  ("NPB") Number of segments per boom ( $1 \leq n \leq 6$ ).

$S_d$  ("SD1") Damper spring constant ratio. This ratio is defined as the damper hinge restraining spring constant  $R_{(1,z,z)}$  divided by the corresponding "gravity gradient spring constant":

$$S_d \triangleq \frac{R_{(1,z,z)}}{[(3 + \sin^2 \delta) I_{(z,z,z)} (\mu_E / a_0^3)]} \quad (B-1)$$

where  $(\mu_E)$  and  $(a_0)$  are defined after Equation (A-46); the angle  $(\delta)$  is  $(\frac{65\pi}{180} - \gamma)$ , where  $(\gamma)$  is the equilibrium yaw angle defined later in this Appendix.  $S_d$  should be greater than unity so that the damper boom will seek a horizontal rest position.

$f_d$  ("FD") Linear damping or non-linear hysteresis\* type damping option at the damper boom hinge. To simulate hysteresis damping, set  $f_d = 0$ . To simulate linear damping set  $f_d$  equal to the desired damping ratio, defined as

$$f_d \triangleq \frac{R'_{(1,z,z)}}{[2 I_{(z,z,z)} \sqrt{(3 + \sin^2 \delta) (S_d - 1) (\mu_E / a_0^3)}]} \quad (B-2)$$

It is noted that this conforms to the standard expression for a damping ratio, with the stiffness term defined as the combined effect of the spring restraint and gravity gradient.

\*The hysteresis damper simulation is described later in this Appendix.

$N_L$  ("NL") Locked mode option. Any or all three degrees of freedom at each hinge may be eliminated, so long as the total number of locked modes  $N_C \leq 36$ . However, only three locked mode configurations are included in the RAE simulation:

$N_L = 1$  Eliminates the rotational degree of freedom about the  $X$  and  $Z$  axes of the damper boom relative to the hub.

$N_L = 2$  Includes  $N_L = 1$  and also locks the torsional degree of freedom at hinges on all antenna boom segments.

$N_L = 3$  Includes  $N_L = 1$  and also locks the three degrees of freedom at the base of each antenna boom. (In this mode,  $n = 1$ ; this simulates a rigid cruciform with a single degree of freedom damper boom).

$I_T$  ("ITHERM") Thermal bending option. To include effects of thermal bending, set  $I_T = 1$ ; otherwise set  $I_T = 0$ .

$N_A$  ("NA") Solar pressure option. To include effects of solar pressure, set  $N_A = 1$ ; otherwise set  $N_A = 0$ .

#### Initial and Final Conditions

$X$  ("XINIT(I)") Twelve initial amplitudes of fundamental RAE satellite librational and flexing modes as defined later in this Appendix.  
 $I = 1, \dots, 12$

$T$  ("ORBS") Total number of orbits to be simulated.

$N_R$  ("ENR") Number of readouts\* printed per orbit.

#### Astronomical Parameters

$e_o$  ("EZ") Eccentricity of orbit

$i_o$  ("EYZ") Inclination angle between the normal to the orbital plane and the north geodetic pole of the celestial sphere.

$\Omega_o$  ("THZ") Longitude of the ascending node measured from the Vernal Equinox.

\*Readout format is described later in this Appendix.

RAE FIXED AND DERIVED INPUTS (PART II)

Hub and Boom Parameters

$m_1$	("EM(1)")	Mass of hub (Kg.)
$l_1$	("EL1")	Effective geometric radius of hub (m.)
$I_{1\alpha\alpha}$	("A(1, $\alpha$ , $\alpha$ )") $\alpha = 1,2,3$	Moments of Inertia about hub X, Y, and Z principal axes respectively (including two dipoles { 18.3 meter length } along hub X -axis)
$m_B$	("EMB")	Boom mass per unit length (Kg./m.)
$l_B$	("ELB")	Total length of each antenna boom (m.)
$l$	("SL")	Length of each segment, $l = l_B / n$
$l_d$	("ELD")	Length of damper boom (m.)
$d$	("DIA")	Boom cross-section diameter (m.)
$\tau$	("THK")	Boom wall thickness (m.)
$\psi$	("OLA")	Boom wall overlap half angle <sup>11</sup> (rad.)
$\nu$	("POR")	Poisson's Ratio
$E$	("E")	Modulus of Elasticity (Newt./m. <sup>2</sup> )
$f_\alpha$	("F( $\alpha$ )") $\alpha = 2,3$	Boom area moments of inertia about the diametral axes parallel to the boom segment Y and Z axis respectively*

$$f_2 = \frac{d^3 \tau}{8} \left[ \pi + \psi + \sin \psi \cos \psi - \frac{2 \sin^2 \psi}{\pi + \psi} \right] \quad (B-3)$$

$$f_3 = \frac{d^3 \tau}{8} \left[ \pi + \psi - \sin \psi \cos \psi \right] \quad (B-4)$$

\*Boom principal axes are in the directions defined in the beginning of this Appendix. The values of  $f_2$  and  $f_3$  are given in Ref. 11 for open slit tubes, but are also valid for any tube with overlap.

$f_1$  ("F(1)") Multiplicative constant for torsional rigidity (locked slit tube):

$$f_1 = \frac{0.5}{1+\nu} (f_2 + f_3) \quad (\text{B-5})$$

$K$  ("CK") Thermal conductivity of boom (Kcal/m.sec. $^{\circ}\text{C}$ )

$e$  ("CTE") Temperature coefficient of linear expansion for boom ( $^{\circ}\text{C}$ ) $^{-1}$

$A_W$  ("AW") Ratio of perforation area to total surface area of the booms.

$J_E$  ("XJE") Earth heat flux density, as given in Eq. (A-15); (Kcal./sec.m $^2$ ).

$J_S$  ("XJS") Solar heat flux density, as given by Eq. (A-16); (Kcal./sec.m $^2$ ).

$a_E$  ————— Boom absorbtivity to Earth radiation. (For the RAE simulation set equal to 0.1 in equation A-19).

$a_S$  ————— Boom absorbtivity to Solar radiation. (For the RAE simulation set equal to 0.05 in equation A-19).

#### Equilibrium Parameters

$K_A, K_B$  ("QA", "QBA") First cantilever mode antenna boom tip deflection in and out of the undeformed cruciform plane respectively (m.)

$\gamma$  ("QGAM") Static yaw angle about hub vertical axis due to skewed damper boom.

These equilibrium parameters, explained in Ref. 12, are used in the computation of initial conditions and readouts described later in this Appendix.

#### Astronomical Parameters

$a_0$  ("AZ") Orbital semi-major axis (m.)

$\omega_0$  ("WZ") Argument of perigee (deg.)

$t_0$  ("TZ") Time at perigee of orbit (sec.). NOTE:  $t \hat{=} 0$  at start of simulation.

$N_D$  ("ND") Vehicle launch date.

## General Program Inputs

Following is a list of System Parameters plus Initial and Final Conditions, as defined in the INTRODUCTION of this report, applicable to the RAE satellite. The Astronomical Parameters, also called for in the INTRODUCTION, are the same as those just defined.

**N** ("N") Total number of rigid members,  $N = 4n + 2$

**m** ("EM(I)") Mass vector with elements  $m_i$ ,  $1 \leq i \leq N$  ( $i^{\text{th}}$  body).

$$m_1 = \text{hub mass}$$

$$m_2 = l_d m_B$$

$$m_i = l m_B \quad \text{for } 3 \leq i \leq N$$

**I** ("A(I,  $\alpha$ ,  $\beta$ )") Inertia tensor with elements  $I(i, \alpha, \beta)$ ,  $1 \leq i \leq N$ ;  $1 \leq \alpha, \beta \leq 3$ :

$$I(i, \alpha, \beta) = 0, \quad \alpha \neq \beta$$

$$I(1, \alpha, \alpha) = \text{hub principal inertias*}$$

$$I(i, 1, 1) = m_i l^2 / 4, \quad 2 \leq i \leq N \quad (\text{B-6})$$

$$I(2, \alpha, \alpha) = m_2 l_d^2 / 12, \quad \alpha = 2, 3 \quad (\text{B-7})$$

$$I(i, \alpha, \alpha) = m_i l^2 / 12, \quad 3 \leq i \leq N; \alpha = 2, 3 \quad (\text{B-8})$$

**R** ("R(J,  $\alpha$ ,  $\beta$ )") Hinge spring constant tensor (See Eqs. A-7 and A-8):

$$R(j, \alpha, \beta), \quad 1 \leq j \leq (N-1); \quad 1 \leq \alpha, \beta \leq 3:$$

$$R(j, \alpha, \beta) = 0, \quad \alpha \neq \beta$$

$$R(1, 1, 1) = R(1, 3, 3) = 0$$

$$R(1, 2, 2) = (3 + \sin^2 \delta) S_d \left( \frac{\mu_E}{a_0^3} \right) I_{(2,2,2)} \quad (\text{B-9})$$

$$R(j, \alpha, \alpha) = (1 - A_w) E f_\alpha / l, \quad 2 \leq j \leq (N-1); \quad 1 \leq \alpha \leq 3 \quad (\text{B-10})$$

\*A considerable saving in machine time was realized by increasing these values in the computational model. Ref. 12 shows that only the highest frequency (lowest amplitude) oscillations are affected.

At this point a brief digression is in order, to explain certain subtle aspects of structural discretization. First it is noted that high frequency torsional oscillations (which consume excessive machine time in simulation) can be circumvented through the previously defined input ( $N_L$ ). When  $N_L \approx 1$  all torsion axes are locked; thus (B-10) is applied for  $\alpha = 2$  and 3 only. When  $N_L = 3$  all antenna joints are locked and (B-10) is bypassed completely. Theoretically the rigidity constants for all locked modes should be zero, since Eq. (A-30) provides the necessary constraint torque. In practice, however, small computational imperfections in the value of this torque are doubly integrated with the dynamical equations. A weak spring and damper have been placed in the locked torsional joints, to counteract this cumulative effect.

In connection with bending moments, Eq. (A-4) was accompanied by a statement that the rate of change of slope ( $d\theta_B/d\ell$ ) cannot in general be adequately determined from a single hinge angle. The inherent accuracy limitations of numerical differentiation can, however, be minimized by using a properly weighted sum to compute derivatives at each point. For the RAE program this was accomplished through augmenting the standard internal torque computation\* as follows: the vector  $\{\lambda \underline{U}\}$  at every antenna boom hinge ( $J_S$ ) is transformed into the co-ordinates of each interacting member ( $I_A$ ); the result, multiplied by the appropriate rigidity matrix  $[R]$  and weighting constant, is included in the total internal moment acting on that member. The members which may interact with

\*The exact form of this refinement will vary with the particular structural topology, but the method exemplified here will be useful for a wide range of applications. It is noted that all weighting constants are set to zero in the Initial Program Setup, (Part 0). Therefore, in the absence of any subsequent introduction of weights in Part I or II, the internal torque modifications in Part IV of the General Program will not invalidate the standard formulation (Eqs. A-7 and A-8) applicable to truly isolated hinges.

any given hinge are the hub and the segments in the same quadrant as the hinge. The extent of interaction is determined from Newton's divided difference formula;<sup>13</sup> a three-segment planar model of an antenna boom will serve to illustrate the technique below.

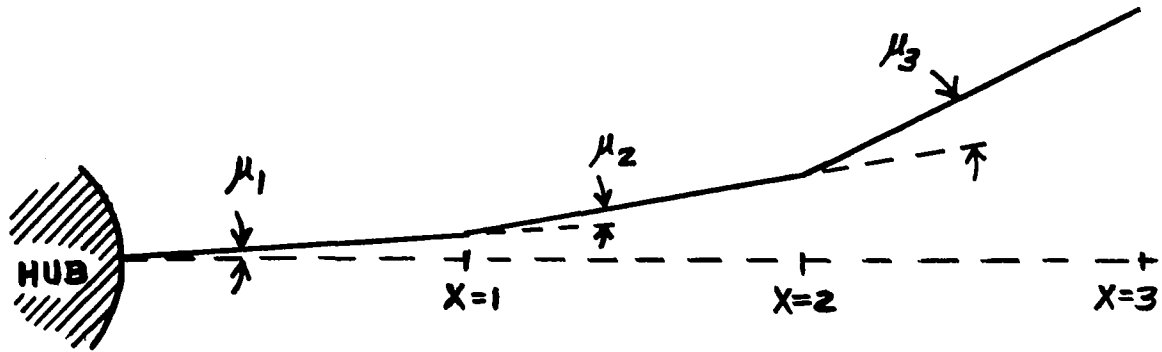


Fig. 4. Segmented Antenna Boom

Normalized Arc Length $X$	Angle off Base Tangent $\theta_B$	1 <sup>st</sup> Divided Difference $f(x_0, x_1)$	2 <sup>nd</sup> Divided Difference $f(x_0, x_1, x_2)$	3 <sup>rd</sup> Divided Difference $f(x_0, x_1, x_2, x_3)$
0	0			
1/2	$\mu_1$	$2\mu_1$	$\frac{2}{3}(\mu_2 - 2\mu_1)$	
3/2	$\mu_1 + \mu_2$	$\mu_2$	$\frac{1}{2}(\mu_3 - \mu_2)$	$\frac{1}{5}\mu_3 - \frac{7}{15}\mu_2 + \frac{8}{15}\mu_1$
5/2	$\mu_1 + \mu_2 + \mu_3$	$\mu_3$	$-\frac{2}{3}\mu_3$	$-\frac{7}{15}\mu_3 + \frac{1}{5}\mu_2$
3	$\mu_1 + \mu_2 + \mu_3$	0		

In the accompanying table, attention is first drawn to the first two columns. The hinge angles ( $\mu$ ) can represent a  $Y$  or  $Z$  axis component of ( $\lambda \underline{U}$ ) in the present problem. For a boom cantilevered to the hub ( $\theta_B$ ) is zero at the



base and, since there should be no bending moment at the free end,  $(\theta_B)$  should not change at  $X = 3$ . In addition to the known values of  $(\theta_B)$  for each segment (presumably the centers), then, these two boundary conditions can be used to determine the derivative of  $(\theta_B)$ . Differentiating Eq. (17) of Ref. 13,

$$f'(X) = f(x_0, x_1) + [2X - (x_0 + x_1)] f(x_0, x_1, x_2) + [3X^2 - 2(x_0 + x_1 + x_2)X + (x_0x_1 + x_0x_2 + x_1x_2)] f(x_0, x_1, x_2, x_3)$$

where  $(\theta_B)$  is to be substituted for  $(f)$  and the divided differences obtained here conform to the definitions in Ref. 13. In solving this equation for  $\theta_B'$  at the hinge points  $X = 0$  and  $X = 1$ , the values  $(0, 1/2, 3/2, 5/2)$  are chosen for  $(x_0, x_1, x_2, x_3)$ , respectively; at  $X = 2$  the values  $(1/2, 3/2, 5/2, 3)$  are used. It is easily verified that

$$f_0' (= \theta_B' @ X = 0) = \frac{46}{15} \mu_1 - \frac{41}{60} \mu_2 + \frac{3}{20} \mu_3$$

$$f_1' (= \theta_B' @ X = 1) = \frac{67}{60} \mu_2 - \frac{2}{15} \mu_1 - \frac{1}{20} \mu_3$$

$$f_2' (= \theta_B' @ X = 2) = \frac{67}{60} \mu_3 - \frac{1}{20} \mu_2$$

The internal moments acting on the hub and the inner, central, and outer segments would then be  $(-f_0')$ ,  $(f_0' - f_1')$ ,  $(f_1' - f_2')$ , and  $(f_2')$ , respectively, multiplied by the appropriate element of  $[R]$ . The amount by which this exceeds the corresponding component of  $\{\lambda[R]U\}$  is provided by the supplemental internal torque computations in Part IV and the weighting coefficients (Fortran designation "EPSIL") in Part II of the program.

The description of General Program inputs will now continue, with the damping tensor as the next item. Aside from the previously mentioned "weak dampers" in the locked modes, the only nonzero value for the present program is

located at the first hinge, its value controlled by the normalized damping ratio ( $f_d$ ) as indicated in Eq. (B-2):

$$R'_{(1,2,2)} = 2 f_d I_{(2,2,2)} \sqrt{(3 + \sin^2 \delta)(S_d - 1) \mu_E / a_0^3} \quad (\text{B-11})$$

and a description of hysteresis damping (for the case  $f_d = 0$ ) appears later in this Appendix.

**S** ("S(I,J)") Structure of the incidence matrix (Note Fig. 3):

$$[S] = \begin{bmatrix} -1 & -1 & -1 & -1 & -1 & 0 \\ 1 & & & & & 0 \\ & 1 & & & & -1 \\ & & 1 & & & -1 \\ & & & 1 & & -1 \\ & & & & 1 & -1 \\ & & & & & 1 \end{bmatrix}$$

(B-12)

$\rho$  ("RHO(J,  $\alpha$ ,  $\beta$ )") Rest position rotation matrix between adjacent bodies with

3 x 3 sub-matrices  $[\rho_j]$ ,  $1 \leq j \leq (N-1)$  :

$$[\rho_1] = [65 \pi / 180]_z$$

$$[\rho_2] = [\pi / 3]_y$$

$$[\rho_3] = [2 \pi / 3]_y$$

(B-13)

$$[\rho_4] = [-2 \pi / 3]_y$$

$$[\rho_5] = [-\pi / 3]_y$$

$$[\rho_j] = [I_{33}], \quad 6 \leq j \leq (N-1)$$

C ("C(I, J)") Hinge connection matrix

$$C_{31} = 3(0.3048); \quad \text{See Fig. 3}$$

$$C_{12} = -C_{13} = -C_{14} = C_{15} = -\frac{1}{2} l_1$$

$$C_{32} = C_{33} = -C_{34} = -C_{35} = \frac{\sqrt{3}}{2} l_1 \quad (\text{B-14})$$

$$C_{ij} = -\frac{1}{2} l_1 \begin{cases} 2 \leq j \leq (N-1), i = 3j + 1 \text{ AND}^* \\ 6 \leq j \leq (N-1), i = 3(j-4) + 1 \end{cases}$$

All other elements of [C] are zero.

\*These values all have the same sign, since the reversal in direction from segment mass center to opposite hinges will be cancelled by the sign reversal in the pertinent incidence matrix elements.

$A_E$  ("AE(I)") Effective areas for solar pressure forces:

If  $N_A = 0$ , all  $A_{E(I)} = 0$ ; otherwise compute the values indicated (See Eqs. A-38 and A-42):

$$A_{E(1)} = \frac{1}{2} \pi l_1^2 \quad (B-15)$$

$$A_{E(2)} = \frac{2}{3} dl_d \quad (B-16)$$

$$A_{E(i)} = \frac{2}{3} dl \quad , \quad 3 \leq i \leq N \quad (B-17)$$

$N_c, m_j$   
("NC", "MI(J)")

Total number of locked hinge degrees of freedom and hinge axis indexing number respectively. Below is a table showing values of  $N_c$  and  $m_j$  for the three locked mode options,  $N_L$ .

$N_L$	$N_c$	$m$
1	2	$m_1 = 1; m_3 = 2$
2	N	$m_1 = 1; m_3 = 2; m_{\{3(J-1)+1\}} = J+1, 2 \leq J \leq N-1$
3	14	$m_1 = 1; m_3 = 2; m_J = J-1, 4 \leq J \leq 15$

$J'_E$  ("XJE") Thermal bending constant for Earth radiation as defined by Eq. (A-19).

$J'_S$  ("XJS") Thermal bending constant for solar radiation as defined by Eq. (A-19).

This completes the RAE System Parameter specifications. The initial conditions need somewhat more detailed treatment here because of their relation to a Lagrangian formulation of the RAE satellite.<sup>12</sup>

Initial values for the angular position { direction cosine matrix  $[\theta_I]$  } and angular velocity vector  $\underline{\omega}_I$  of each member I of the discrete RAE satellite model are derived from the initial conditions of an equivalent flexible continuous RAE satellite model.<sup>12</sup> First cantilever mode shape amplitudes of the booms are linearly transformed into a set of "satellite modes" ( $X_5 \cdots X_{12}$ ). It is of interest to excite these "satellite modes" separately or in combination in the discrete model program. Also, nonzero initial values of the libration Euler angles ( $X_1, X_2, X_3$ ) with respect to the local frame and of the single degree of freedom damper angle ( $X_4$ ) from the continuous model will excite similar motion in the discrete model. Thus the initial values of the twelve quantities ( $X_1 \cdots X_{12}$ ) are transformed to the initial attitude of each member in the discrete model. It is noted that there is no loss of generality in setting the initial derivatives ( $\dot{X}_1 \cdots \dot{X}_{12}$ ) to zero, since motion is still excited by initial displacements from equilibrium.

The transformation from the twelve variables of the continuous model to each member's attitude in the discrete model is accomplished separately for the hub and the damper boom, and in combination for the antenna boom segments. First, the orthogonal transformation from hub to local axes is written as

$$[\theta_1] = [X_2]_y [X_1]_x [X_3 + \delta]_z \quad (B-18)$$

where  $X_1, X_2$ , and  $X_3$  are the roll, pitch, and yaw libration angles respectively and  $\delta$  is a static yaw angle of the hub body axes in equilibrium due to the skewed

damper boom. The orthogonal transformation from damper principal axes to the local frame is

$$[\theta_2] = [\theta_1][\rho_1]^T[X_4]_y \quad (\text{B-19})$$

where  $[\rho_1]$  represents the 65 degree hub-to-damper transformation about the yaw axis (see Fig. 3).

The conversion from the generalized coordinates describing the satellite deformation modes to any boom segment direction cosine matrix can be separated into three steps:

1. First, all in-plane and out of plane tip deflections can be expressed as a linear combination of the satellite flexing mode amplitudes. For example the in-plane and out of plane tip deflections of the lower left antenna boom are

$$W_z = -\frac{1}{2} [X_6 + (X_8 + 2K_A) - X_9 - X_{11}] \quad (\text{B-20})$$

and

$$W_y = \frac{1}{2} [X_5 + (X_7 + 2K_B) - X_{10} - X_{12}] \quad (\text{B-21})$$

where  $K_A$  and  $K_B$  are the in and out of plane static (equilibrium) tip deflections, respectively. All other boom tip deflections follow in a similar fashion from the transformation defined in Ref. 12.

2. In the second step, the elastic deformation slope is computed for each segment, making use of the first cantilever mode shape. A question immediately arises as to the method of fitting a finite number of segments to the cantilever curve. The segments could be inscribed or circumscribed, or their mass centers could be matched to the mode shape function; alternatively, the slope of each segment could be chosen to match the corresponding portion of strain energy in the continuous

elastic curve. Actually, the accompanying Fortran listing uses none of these methods. Instead, the first cantilevered mode function was approximated by a least squares fit, giving rise to proportionality constants ( $A_k$ ; Fortran designation "SLSQ") which fix the slopes of the  $k^{\text{th}}$  segment as

$$\Delta y = A_k W_z / l_B, \quad 1 \leq k \leq n \quad (\text{B-22})$$

and

$$\Delta z = A_k W_y / l_B, \quad 1 \leq k \leq n \quad (\text{B-23})$$

for any values of in-plane ( $W_z$ ) and transverse ( $W_y$ ) tip deflection. It was then found that, for three\* segments per boom, the results could be improved through small changes in the relative magnitudes of ( $A_k$ ). Chosen values for this case (i.e.,  $n = 3$ ) minimized the initial angular accelerations under equilibrium conditions. No further improvements were investigated for other segmented approximations, but curve fitting is recognized as a possible means of improving future discretized structural models of this type.

3. Finally, the transformation is computed for segment-to-local coordinates. Again using the lower left antenna quadrant as an example,

$$[\theta_7] = [\theta_1][\rho_2]^T[\Delta] \quad (\text{B-24})$$

where  $[\Delta]$  is computed exactly as in Eq. (A-21) using the angles in (B-22) and (B-23).

---

\*A three-segment model was chosen for actual run trials, as a compromise between accuracy and economy of computation.

Initial angular rates arise solely from orbital motion since, as previously explained, the initial generalized co-ordinate derivatives ( $\dot{X}_1, \dot{X}_2, \dots, \dot{X}_{12}$ ) are zero. For any member, then, the initial angular rate vector is

$$\underline{\omega}_I = \dot{v} [\theta_I]^T \underline{1}_2, \quad 1 \leq I \leq N \quad (\text{B-25})$$

where ( $\dot{v}$ ) follows readily from Eq. (A-52).



## HYSTERESIS DAMPER SIMULATION

The hysteresis damping torque for the RAE satellite is taken from the model found in Ref. 14. The damping torque equation, repeated here, is

$$T_H = T_R + 2 T_P [1 - \exp\{-\Sigma |\lambda - \lambda_R|\}] \operatorname{sgn}(\dot{\lambda}) \quad (\text{B-26})$$

where:

$T_R$  = damping torque at the time when  $\dot{\lambda}$  last changed sign,

$T_P$  = peak (saturation) damper torque,

$\Sigma$  = exponential rate constant,

$\lambda$  = angle between damper axis and damper rest position (i.e.,  $X_4$  in the problem at hand),

$\lambda_R$  = damper angle when  $\dot{\lambda}$  last changed sign.

The damper hinge has only one rotational degree of freedom (y-axis of the damper boom). The other two degrees of freedom are eliminated by locked modes as described in Appendix A. When the input variable  $f_d$  is set to zero, this hysteresis torque replaces the usual (linear) computation for damping torques in part IV.



- (2) When the sightline from the satellite to the sun is not obstructed by the Earth, this will be indicated by the readout "IN SUN"; the readout "SHADOW" appears during eclipse.
- (3) Attitude of the reference axes of the composite satellite with respect to local axes,

$$[\theta'] = [\theta_1] [-\gamma]_{\underline{z}} \quad (B-27)$$

where  $\gamma$  is the static offset angle of the  $\underline{X}_{HUB} - \underline{Z}_{HUB}$  plane with the orbital plane:

"ATTITUDE"		
$\theta'_{11}$	$\theta'_{12}$	$\theta'_{13}$
$\theta'_{21}$	$\theta'_{22}$	$\theta'_{23}$
$\theta'_{31}$	$\theta'_{32}$	$\theta'_{33}$

- (4) Attitude of the damper boom with respect to its reference position:

$$[v] = [P_1] [\theta_1]^T [\theta_2] \quad (B-28)$$

"DAMPER"	$v_{23}$	$v_{31}$	$v_{12}$
----------	----------	----------	----------

- (5) Antenna boom deformation is characterized by lateral deflections, both in and out of the cruciform reference plane, for the tip of each segment. The in-plane and out-of-plane deflections are the 3rd and 2nd components respectively of a deflection vector  $\underline{d}_i$ , where ( $i$ ) is the segment index number. Since the deflection at the tip of any segment includes the deflections

of all inner segments,  $\underline{d}$  can be computed by a recursion formula:

$$\underline{d}_{4j+k-2} = \underline{d}_{4(j-1)+k-2} + l [r_{k+1}] [\theta_1]^T \begin{bmatrix} \theta_{4j+k-2,11} \\ \theta_{4j+k-2,21} \\ \theta_{4j+k-2,31} \end{bmatrix} \quad (B-29)$$

$$2 \leq j \leq n; 1 \leq k \leq 4$$

where  $j$  is the index number of the segment tip. To start the recursion, the values of  $\underline{d}_3$ ,  $\underline{d}_4$ ,  $\underline{d}_5$ , and  $\underline{d}_6$  are computed from the last term of the same expression, (B-29). The relative twist angle (rad.) between adjacent members is computed from the trace angle ( $\lambda$ ) and the X-axis component of the deformation eigenvector  $\underline{U}$  for the hinge connecting those members; ( $\lambda$ ) and  $\underline{U}$  are defined in Eqs. (A-2) and (A-3), respectively.

$$d_{i,1} = \lambda U_1, \quad 3 \leq i \leq N \quad (B-30)$$

The "DEFORMATION" format is as follows:

Boom number (K)	1	2	3	4
"IN-PLANE"	$d_{33}$	$d_{43}$	$d_{53}$	$d_{63}$
	$d_{73}$	$d_{83}$	$d_{93}$	$d_{10,3}$
	$\vdots$	$\vdots$	$\vdots$	$\vdots$
"OUT OF PLANE"	$d_{32}$	$d_{42}$	$d_{52}$	$d_{62}$
	$d_{72}$	$d_{82}$	$d_{92}$	$d_{10,2}$
	$\vdots$	$\vdots$	$\vdots$	$\vdots$

"TWIST"	$d_{31}$	$d_{41}$	$d_{51}$	$d_{61}$
	$d_{71}$	$d_{81}$	$d_{91}$	$d_{10,1}$
	$\vdots$	$\vdots$	$\vdots$	$\vdots$
	$\vdots$	$\vdots$	$\vdots$	$\vdots$

(6) The amplitudes of the satellite flexing modes<sup>12</sup> are computed from the antenna boom tip deflections and printed out. The computation is the exact inverse of the operation used to find tip deflections from flexing mode amplitudes, described earlier in this Appendix.

For example, the in-plane neutral mode amplitude is:

$$X_8 = -\frac{1}{2} (d_{4n+1,3} - d_{4n+2,3} + d_{4n-1,3} - d_{4n,3}) - 2K_A \quad (\text{B-31})$$

The "SATELLITE MODES" format is as follows:

"ROLL" ( $X_5$ ) "PITCH" ( $X_6$ ) "YAW" ( $X_7$ )

"LONGITUDINAL" ( $X_9$ ) "LATERAL" ( $X_{10}$ ) "VERTICAL" ( $X_{11}$ )

"IN-PLANE NEUTRAL" ( $X_8$ ) "OUT OF PLANE NEUTRAL" ( $X_{12}$ )

APPENDIX C  
PROGRAM LISTING

The RAE segmented model program presented here has been successfully run in Fortran IV single precision on the Univac 1108 and has been found in agreement with the independent Lagrangian analysis of Ref. 12. While many of the Fortran statements are self-explanatory or follow readily from previous discussion, understanding of the overall computational scheme is enhanced in several instances by the accompanying comments, referrals to equations, cross-references between different parts of the program, etc. It will be reiterated here that usage of the program for other satellite configurations will not require knowledge of the material in these Appendices. Program utilization for general purposes calls for 1) all inputs specified in the INTRODUCTION of this report, and 2) Parts 0, III, and IV of the present listing (with present FORMAT and WRITE statements replaced by desired readouts for the particular problem under consideration\*), augmented by the accompanying subroutines ICE, INTEC, INVERT, and XSIMEQ, plus card Nos. 55-58 which provide necessary zero resets for each program run. It should be noted that the hinge interactions, solar pressure forces, thermal bending, and hysteresis damping present in Part IV, unless actuated by inputs in Parts I and II, are de-activated by the cards at the end of Part 0. If similar effects are to be included in a simulation for another satellite configuration, the following minor modifications are needed:

(1) Elastic coefficients derived on pages 38-40 must be co-ordinated with the appropriate satellite geometry, necessitating logic changes in cards 818-848.

\*Note that deletion of the computations associated with readouts in the present program (e.g., calculations involving the Fortran designation "SD") is optional.

(2) The geometry of each member will determine its response to solar radiation pressure; card Nos. 646-652 will be replaced accordingly if solar pressure effects are to be taken into account.

(3) The thermal bending formulation was derived in terms of lengths between centers of adjacent members (See discussion preceding Eq. A-10). When this is not uniform throughout the structure, simple logic must be introduced into the computation (for the RAE this is done by card Nos. 722-724).

(4) Nonlinear damping and/or spring action can easily be simulated by modifying the internal torque ("EL") computation at any hinge.





```

43         KBBC = 0
44         WRITE (6,1971) STP1 _____ Readout for numerical integration step size.
45         1971 FORMAT (1H1E18.5)
46         1970 CONTINUE
47         READ (5,190) NL,NA,ITHERM,NPB,THZ,EYZ,EZ,ENR,DRBS,FD,SD1
48         190  FORMAT (4I1,7F10.0)
49         READ (5,1901) XINIT
50         1901 FORMAT (6F10.0)
51         IF (NL .EQ. 3) NPB = 1 _____ Antenna base lock is allowed only for the rigid cruciform.
52
53         C
54         C           PART II
55         C
56         DO 1031 J=1,38
57         GAM(J) = 0.0
58         DO 1031 I=1,78
59         1031 SQU(I,J) = 0.0
60         DO 1032 I=1,26
61         DO 1032 J=1,3
62         1032 SD(I,J) = 0.0
63         DO 1029 J = 1,6
64         1029 SLSQ(J) = 0.
65         GO TO (1038,1033,1034,1035,1036,1037),NPB _____ See pages 45-46.
66         1033 SLSQ(1) = .595386
67         SLSQ(2) = 1.40461
68         GO TO 1038
69         1034 CONTINUE
70         SLSQ(1) = .5461
71         SLSQ(2) = 1.1432
72         SLSQ(3) = 1.3107
73         GO TO 1038
74         1035 SLSQ(1) = .321406
75         SLSQ(2) = 1.01717
76         SLSQ(3) = 1.28445
77         SLSQ(4) = 1.37697
78         GO TO 1038
79         1036 SLSQ(1) = .261152
80         SLSQ(2) = .865497
81         SLSQ(3) = 1.1645
82         SLSQ(4) = 1.33302
83         SLSQ(5) = 1.37583
84         GO TO 1038
85         1037 SLSQ(1) = .21987
86         SLSQ(2) = .750147

```

56

Obtained from minimum initial  $|d\omega/dt|$  at equilibrium;  
slopes for 2, 4, 5 or 6 segments were obtained by least squares.

```

86      SLSQ(3) = 1.04962
87      SLSQ(4) = 1.25421
88      SLSQ(5) = 1.34979
89      SLSQ(6) = 1.37636
90 1038 CONTINUE
91      SIGH = 77.
92      TPH=.4506
93      TRH = 0.0
94      AMBDR = 0.0
95      SDD = 1.0
96      AMDDT = 0.
97      XJS = 3.0E+08*SPC/4184.
98      XJE = 5.67E-08*246.0**4/4184.
99      DO 11000 I=1,6
100     DO 11000 J=1,7
101 11000 EPSIL(I,J) = 0.0
102     GO TO (11004,11008,11005,11006,11007,11009),NPB
103 11C08 EPSIL(1,1) = -13./6.
104     EPSIL(1,2) = 7./3.
105     EPSIL(1,3) = -1./6.
106     EPSIL(2,1) = 5./6.
107     EPSIL(2,2) = -1.
108     EPSIL(2,3) = 1./6.
109     GO TO 11004
110 11005 CONTINUE
111     EPSIL(1,1) = -31./15.
112     EPSIL(1,2) = 11./5.
113     EPSIL(1,3) = -2./15.
114     EPSIL(2,1) = 41./60.
115     EPSIL(2,2) = -4./5.
116     EPSIL(2,3) = 1./6.
117     EPSIL(2,4) = -1./20.
118     EPSIL(3,1) = -3./20.
119     EPSIL(3,2) = 1./5.
120     EPSIL(3,3) = -1./6.
121     EPSIL(3,4) = 7./60.
122     GO TO 11004
123 11006 CONTINUE
124     EPSIL(1,1) = -31./15.
125     EPSIL(1,2) = 11./5.
126     EPSIL(1,3) = -2./15.
127     EPSIL(2,1) = 41./60.
128     EPSIL(2,2) = -4./5.

```

Damper exponential constant.

This normalized hysteresis saturation torque (equivalent to the net spring torque on an isolated damper, skewed at 65° and inclined at 0.4506 radian) when expressed in English units corresponds to  $1.05 \times 10^{-3}$  ft.lb. - See card No. 461.

} Hysteresis  
 } damper  
 } initialization

Eq. A-16.

Eq. A-15.

See page 40.

```
129      EPSIL(2,3) = 19./120.
130      EPSIL(2,4) = -1./24.
131      EPSIL(3,1) = -3./20.
132      EPSIL(3,2) = 1./5.
133      EPSIL(3,3) = -2./15.
134      EPSIL(3,4) = 2./15.
135      EPSIL(3,5) = -1./20.
136      EPSIL(4,3) = 1./24.
137      EPSIL(4,4) = -19./120.
138      EPSIL(4,5) = 7./60.
139      GO TO 11004
140 11007 CONTINUE
141      EPSIL(1,1) = -31./15.
142      EPSIL(1,2) = 11./5.
143      EPSIL(1,3) = -2./15.
144      EPSIL(2,1) = 41./60.
145      EPSIL(2,2) = -4./5.
146      EPSIL(2,3) = 19./120.
147      EPSIL(2,4) = -1./24.
148      EPSIL(3,1) = -3./20.
149      EPSIL(3,2) = 1./5.
150      EPSIL(3,3) = -2./15.
151      EPSIL(3,4) = 1./8.
152      EPSIL(3,5) = -1./24.
153      EPSIL(4,3) = 1./24.
154      EPSIL(4,4) = -1./8.
155      EPSIL(4,5) = 2./15.
156      EPSIL(4,6) = -1./20.
157      EPSIL(5,4) = 1./24.
158      EPSIL(5,5) = -19./120.
159      EPSIL(5,6) = 7./60.
160      GO TO 11004
161 11009 EPSIL(1,1) = -31./15.
162      EPSIL(1,2) = 11./5.
163      EPSIL(1,3) = -2./15.
164      EPSIL(2,1) = 41./60.
165      EPSIL(2,2) = -4./5.
166      EPSIL(2,3) = 19./120.
167      EPSIL(2,4) = -1./24.
168      EPSIL(3,1) = -3./20.
169      EPSIL(3,2) = 1./5.
170      EPSIL(3,3) = -2./15.
171      EPSIL(3,4) = 1./8.
```

172 EPSIL(3,5) = -1./24.  
 173 EPSIL(4,3) = 1./24.  
 174 EPSIL(4,4) = -1./8.  
 175 EPSIL(4,5) = 1./8.  
 176 EPSIL(4,6) = -1./24.  
 177 EPSIL(5,4) = 1./24.  
 178 EPSIL(5,5) = -1./8.  
 179 EPSIL(5,6) = 2./15.  
 180 EPSIL(5,7) = -1./20.  
 181 EPSIL(6,5) = 1./24.  
 182 EPSIL(6,6) = -19./120.  
 183 EPSIL(6,7) = 7./60.  
 184 11004 CONTINUE  
 185 TZ = 0.0  
 186 WZ = 0.0  
 187 AZ = 0.1238E+08 \_\_\_\_\_ Semimajor axis for 6000 Km. altitude.  
 188 ND = 80 \_\_\_\_\_ March 21.  
 189 ENPB = NPB  
 190 C  
 191 C FAIRCHILD BOOM  
 192 C  
 193 ELB = 750.\*.3048 \_\_\_\_\_ Antenna length in meters.  
 194 103 SL = ELB/ENPB \_\_\_\_\_ Segment length.  
 195 THK = .508E-04 \_\_\_\_\_ Boom wall thickness.  
 196 E = .117E+12  
 197 3418 AW = 0.0 \_\_\_\_\_ Value of E used in Eq. B-10 includes effects of perforations.  
 198 POR = 0.3 \_\_\_\_\_ Poisson's ratio.  
 199 EMB = 0.480E-03\*14.5939/0.3048 \_\_\_\_\_ Linear mass density of booms (kg./m.).  
 200 CK = 0.031 \_\_\_\_\_ Thermal conductivity of booms (page 36).  
 201 DIA = 0.587/39.37  
 202 OLA = 0.1 \_\_\_\_\_ Small overlap angle due to interlocking at seam; not critical.  
 203 CTE = 0.0  
 204 IF (ITHERM .NE. 0) CTE = 1.87E-05 \_\_\_\_\_ coefficient of thermal expansion.  
 205 F(2) = .125\*DIA\*\*3\*THK\*(PI+OLA+SIN(OLA)\*COS(OLA)-2.0\*SIN(OLA)\*\*2/  
 206 1(PI+OLA)) \_\_\_\_\_ Eq. B-3.  
 207 F(3) = .125\*DIA\*\*3\*THK\*(PI+OLA-SIN(OLA)\*COS(OLA)) \_\_\_\_\_ Eq. B-4.  
 208 F(1) = 0.5/(1+POR)\*[F(2)+F(3)] \_\_\_\_\_ Eq. B-5.  
 209 DO 104 I = 1,3  
 210 104 F(I) = E\*F(I)\*(1.0-AW)/SL \_\_\_\_\_ Eq. B-10; see card No. 368.  
 211 XJE = ELB/4.0/ENPB/CK/THK\*0.1\*CTE\*DIA\*XJE } \_\_\_\_\_ Eq. A-19.  
 212 XJS = ELB/4.0/ENPB/CK/THK\*.05\*CTE\*DIA\*XJS }  
 213 N = 4\*NPB+2 \_\_\_\_\_ Segments, hub, and damper.  
 214 N3 = 3\*N

```

215      NM = N-1
216      EEE1=1.0E-06/2.0
217      EEE2=1.0E-04/2.0
218      DO 5555 I=1,N3
219 5555  ERL(I) = EEE1
220      N12 = 12*N
221      NNNN = N3+1
222      DO 5556 I=NNNN,N12
223 5556  ERL(I) = EEE2
224      DANG = 65.*PI/180.
225      QKA = 35.57
226      QBA = .9830
227      QGAM = .1131
228      DO 7301 I=1,75
229 7301  MI(I) = 0
230      GO TO (7303,7304,7305),NL
231 7303  NC = 2
232      MI(1) = 1
233      MI(3) = 2
234      GO TO 7401
235 7304  NC = N
236      MI(1) = 1
237      MI(3) = 2
238      DO 7307 I=2,NM
239      M = 3*(I-1)+1
240 7307  MI(M) = I+1
241      GO TO 7401
242 7305  NC = 14
243      QKA = 0.0
244      QBA = 0.0
245      QGAM = .0623134
246      MI(1) = 1
247      MI(3) = 2
248      DO 7308 I=4,15
249 7308  MI(I) = I-1
250 7401  CONTINUE
251      EL1 = 1.5*0.3048
252      ELD = CBRT(12./EMB*1.0E+04*14.5939*.3048**2)
253      EM(1) = 10.52*14.5939
254      EM(2) = ELD*EMB
255      DO 105 I = 3,N
256 105   EM(I) = ELB*EMB/ENPB
257      DO 106 I = 1,N

```

Allowable error per integration step for angular rates (rad./sec).

Allowable error per integration step for direction cosines.

Angle  $\theta_D$  of Ref. 12; damper skew angle.

Equilibrium parameters (Ref. 12, Case 2).

See pages 34 and 43.

Values for rigid cruciform.

Assumed hub dimension; not at all critical.

Damper length corresponding to  $10^4$  slug-ft.<sup>2</sup>

```

258 DO 106 J = 1,3
259 DO 106 K = 1,3
260 106 A(I,J,K) = 0.0
261 A(1,1,1) = 14.24
262 A(1,2,2) = 90.8
263 A(1,3,3) = 92.68
264 A(1,1,1) = A(1,1,1)*1000.
265 A(1,2,2) = A(1,2,2)*200.
266 A(1,3,3) = A(1,3,3)*20. } See footnote on page 37.
267 1065 CONTINUE
268 DO 107 I = 1,3
269 107 A(1,I,I) = A(1,I,I)*14.5939*0.3048**2
270 A(2,1,1) = EM(2)*DIA**2/4.0 Eq. B-6.
271 A(2,1,1) = A(2,1,1)*10000.
272 DO 108 I = 2,3
273 108 A(2,I,I) = 1./12.*EM(2)*ELD**2 Eq. B-7.
274 DO 109 I = 3,N
275 A(I,1,1) = EM(I)*DIA**2/4.0 Eq. B-6.
276 A(I,1,1) = A(I,1,1)*10000. Artificial enlargement of small inertias.
277 DO 109 J = 2,3
278 109 A(I,J,J) = 1./12.*EM(I)*SL**2 Eq. B-8.
279 IF(NA) 110,111,110
280 111 DO 112 I = 1,N
281 112 AE(I) = 0.0
282 GO TO 114
283 110 AE(1) = 0.5*PI*EL1**2 Sphere; Eq. B-15.
284 AE(2) = 2./3.*DIA*ELD Cylinder; Eq. B-16.
285 DO 113 I = 3,N
286 113 AE(I) = 2./3.*DIA*SL Cylinder; Eq. B-17.
287 114 M = N-1
288 DO 115 I = 1,N
289 DO 115 J = 1,M
290 115 S(I,J) = 0.0
291 DO 116 I = 1,5
292 116 S(I,I) = -1.0
293 IF (NPB .EQ. 1) GO TO 5070
294 DO 117 I = 6,M
295 J = I-3
296 117 S(J,I) = -1.0
297 5070 CONTINUE
298 DO 118 I = 1,M
299 J = I+1
300 118 S(J,I) = 1.0

```

```

301      M = 3*N
302      DO 119 I = 1,M
303      DO 119 J = 1,M
304 119   C(I,J) = 0.0
305      C(3,1) = 3.0*0.3048
306      C(1,2) = -0.5*EL1
307      C(1,5) = C(1,2)
308      C(1,3) = -C(1,2)
309      C(1,4) = C(1,3)
310      C(3,4) = -EL1*SIN(PI/3.)
311      C(3,5) = C(3,4)
312      C(3,2) = -C(3,4)
313      C(3,3) = C(3,2)
314      M = N-1
315      DO 120 I = 2,M
316      K = 3*I+1
317 120   C(K,I) = -SL/2.
318      IF (NPB .EQ. 1) GO TO 5071
319      DO 121 J = 6,M
320      K = 3*(J-4)+1
321 121   C(K,J) = -SL/2.
322 5071  CONTINUE
323      DO 122 I = 1,M
324      DO 122 J = 1,3
325      DO 122 K = 1,3
326 122   RHO(I,J,K) = 0.0
327      RHO(1,1,1) = COS(DANG)
328      RHO(1,2,2) = COS(DANG)
329      RHO(1,1,2) = SIN(DANG)
330      RHO(1,2,1) = -RHO(1,1,2)
331      RHO(1,3,3) = 1.
332      RHO(2,2,2) = 1.
333      RHO(3,2,2) = 1.
334      RHO(4,2,2) = 1.
335      RHO(5,2,2) = 1.
336      RHO(2,1,1) = .5
337      RHO(2,3,3) = .5
338      RHO(5,1,1) = .5
339      RHO(5,3,3) = .5
340      RHO(3,1,1) = -.5
341      RHO(3,3,3) = -.5
342      RHO(4,1,1) = -.5
343      RHO(4,3,3) = -.5

```

Eq. B-14. Note: Damper displacement  $C_{31}$  below hub mass center is not at all critical.

Eq. B-13.

```

344      RHO(2,3,1) = SIN(PI/3.)
345      RHO(3,3,1) = SIN(PI/3.)
346      RHO(4,1,3) = SIN(PI/3.)
347      RHO(5,1,3) = SIN(PI/3.)
348      RHO(2,1,3) = -SIN(PI/3.)
349      RHO(3,1,3) = -SIN(PI/3.)
350      RHO(4,3,1) = -SIN(PI/3.)
351      RHO(5,3,1) = -SIN(PI/3.)
352      IF (NPB .EQ. 1) GO TO 5072
353      DO 123 I = 6,M
354      DO 123 K = 1,3
355      123 RHO(I,K,K) = 1.
356      5072 CONTINUE
357      M = N-1
358      DO 127 I = 1,M
359      DO 127 J = 1,3
360      DO 127 K = 1,3
361      R(I,J,K) = 0.0
362      127 RP(I,J,K) = 0.0
363      IF (NL .EQ. 3) GO TO 5073 _____ Rigid Cruciform.
364      IQL = 1
365      IF (NL .EQ. 2) IQL = 2 _____ Locked torsional modes.
366      DO 128 I=2,M
367      DO 128 J=IQL,3
368      128 R(I,J,J) = F(J) _____ See card No. 210.
369      IF (NL .NE. 2) GO TO 1289
370      5073 CONTINUE
371      DO 1288 I=1,NM
372      R(I,1,1) = 10.*A(I+1,2,2)*FMU/AZ**3
373      RP(I,1,1) = 5.*A(I+1,2,2)*SQRT(FMU/AZ**3) } _____ Weak springs and dampers for locked torsional
374      1288 CONTINUE
375      1289 CONTINUE
376      R(1,2,2) = SD1*(3.0+SIN(DANG -QGAM)**2)*FMU/AZ**3*A(2,2,2)
377      RP(1,2,2) = 2.0*FD*A(2,2,2)*SQRT(3.0+SIN(DANG -QGAM)**2)*
378      1((SD1-1.0)*FMU/AZ**3) _____ Eq. B-11.
379      DUR(2,2) = R(2,2,2) } _____ Used for interacting hinges.
380      DUR(3,3) = R(2,3,3) }
381      XC = COS(XINIT(1))
382      YC = COS(XINIT(2))
383      ZC = COS(QGAM+XINIT(3))
384      XF = SIN(XINIT(1))
385      YF = SIN(XINIT(2))
386      ZF = SIN(QGAM+XINIT(3))

```

Eq. B-13.

Eq. B-9 (at  $S_1 = 1.298$  this provides a damper spring constant of 0.01015 ft.-lb./radian).



```

387      TH(1,1,1) = ZC*YC-XF*YF*ZF
388      TH(1,1,2) = ZF*YC+XF*YF*ZC
389      TH(1,1,3) = -XC*YF
390      TH(1,2,1) = -XC*ZF
391      TH(1,2,2) = XC*ZC
392      TH(1,2,3) = XF
393      TH(1,3,1) = ZC*YF+XF*YC*ZF
394      TH(1,3,2) = YF*ZF-XF*YC*ZC
395      TH(1,3,3) = XC*YC
396      TH(2,1,1) = COS(XINIT(4))
397      TH(2,1,2) = 0.0
398      TH(2,1,3) = -SIN(XINIT(4))
399      TH(2,2,1) = 0.0
400      TH(2,2,2) = 1.0
401      TH(2,2,3) = 0.0
402      TH(2,3,1) = SIN(XINIT(4))
403      TH(2,3,2) = 0.0
404      TH(2,3,3) = COS(XINIT(4))
405      DO 7480 I=1,3
406      DO 7480 J=1,3
407      DVEC(I,J) = 0.0
408      DO 7480 K=1,3
7480      DVEC(I,J) = DVEC(I,J)+RHO(1,K,I)*TH(2,K,J)
410      DO 7481 I=1,3
411      DO 7481 J=1,3
412      TH(2,I,J) = 0.0
413      DO 7481 K=1,3
7481      TH(2,I,J) = TH(2,I,J)+TH(1,I,K)*DVEC(K,J)
415      XINIT(7) = XINIT(7)+2.0*QBA
416      XINIT(8) = XINIT(8)+2.0*QKA
417      ZIN(1) = -0.5*(XINIT(6)+XINIT(8)-XINIT(9)-XINIT(11))
418      ZIN(2) = -0.5*(XINIT(6)-XINIT(8)-XINIT(9)+XINIT(11))
419      ZIN(3) = -0.5*(XINIT(6)+XINIT(8)+XINIT(9)+XINIT(11))
420      ZIN(4) = -0.5*(XINIT(6)-XINIT(8)+XINIT(9)-XINIT(11))
421      YIN(1) = 0.5*(XINIT(5)+XINIT(7)-XINIT(10)-XINIT(12))
422      YIN(2) = -0.5*(-XINIT(5)+XINIT(7)+XINIT(10)-XINIT(12))
423      YIN(3) = -0.5*(XINIT(5)+XINIT(7)+XINIT(10)+XINIT(12))
424      YIN(4) = 0.5*(-XINIT(5)+XINIT(7)-XINIT(10)+XINIT(12))
425      DO 1812 K=1,4
426      DO 1812 J=1,NPB
427      I = 4*J-2+K
428      YYY = SLSQ(J)*ZIN(K)/ELB
429      ZZZ = SLSQ(J)*YIN(K)/ELB

```

Eq. B-18.

Eq. B-19.

Eq. B-20.

Eq. B-21.

Eq. B-22.

Eq. B-23.

```

430      YYS = YYY**2
431      ZZS = ZZZ**2
432      SQUR = SQRT(1.0-YYS-ZZS)
433      TH(I,1,1) = SQUR
434      TH(I,1,2) = -ZZZ
435      TH(I,1,3) = -YYY
436      TH(I,2,1) = ZZZ
437      TH(I,2,2) = (YYS+ZZS*SQUR)/(YYS+ZZS)
438      TH(I,2,3) = YYY*ZZZ*(SQUR-1.0)/(YYS+ZZS)
439      TH(I,3,1) = YYY
440      TH(I,3,2) = TH(I,2,3)
441      TH(I,3,3) = (ZZS+YYS*SQUR)/(YYS+ZZS)
442      IF (YYS+ZZS .LT. 1.E-30) TH(I,2,2) = 1.0 }
443      IF (YYS+ZZS .LT. 1.E-30) TH(I,3,3) = 1.0 }  Resolution of possible singularity.
444      DO 1813 II=1,3
445      DO 1813 JJ=1,3
446      DVEC(II,JJ) = 0.0
447      DO 1813 KK=1,3
448      1813 DVEC(II,JJ) = DVEC(II,JJ)+RHO(K+1,KK,II)*TH(I,KK,JJ)
449      DO 1814 II=1,3
450      DO 1814 JJ=1,3
451      TH(I,II,JJ) = 0.0
452      DO 1814 KK=1,3
453      1814 TH(I,II,JJ) = TH(I,II,JJ)+TH(1,II,KK)*DVEC(KK,JJ)
454      1812 CONTINUE
455      DO 1815 I=1,N
456      DO 1815 J=1,3
457      CAM = -SQRT(FMU)*TZ/AZ**1.5
458      1815 WM(J,I) = TH(I,2,J)*SQRT(FMU)/AZ**1.5*(1.0+2.0*EZ*COS(CAM)
459      1 +2.5*EZ**2*COS(2.0*CAM)+1.0/12.0*EZ**3*(39.*COS(3.0*CAM)-3.0*
460      1 COS(CAM))) } Eq. B-25.
461      TPH = TPH*(SD1-1.0)*(3.+SIN(DANG -QGAM)**2)*A(2,2,2)*FMU/AZ**3 } See card Nos. 92 and 376.
462      WRITE (6,4916)
463      4916 FORMAT (1H130X33HRAE SATELLITE DYNAMICS SIMULATION)
464      WRITE (6,4918) NPB,NL,E
465      4918 FORMAT (1H022X19HFAIRCHILD BOOMS OF I1,19H SEGMENTS PER BOOM. 5X
466      15HNL = I3,5X4HE = E10.4)
467      IF (ITHERM .NE. 0) WRITE (6,4919)
468      4919 FORMAT (1H034X24HTHERMAL EFFECTS INCLUDED)
469      IF (NA .NE. 0) WRITE (6,4920)
470      4920 FORMAT (1H029X31HSOLAR PRESSURE EFFECTS INCLUDED)
471      WRITE (6,4921) SD1,FD
472      4921 FORMAT (1H020X22HDAMPER SPRING CONSTANT E12.4,5X13HDAMPING RATIO

```

```

473      1E12.4)
474      WRITE (6,4922) AZ,THZ,EYZ,EZ,ENR
475  4922 FORMAT (1H016X5HORBIT5X1HAE12.5,5X1HOE12.5,5X1HIE12.5,5X1HEE12.5,
476      1 5X5HNR = F3.0)
477      WRITE (6,4923)   ORBS
478  4923 FORMAT (1H030X19HSIMULATION TO LAST F6.3,7H ORBITS)
479      XINIT(7) = XINIT(7)-2.*QBA
480      XINIT(8) = XINIT(8)-2.*QKA
481      WRITE (6,4924) (I,XINIT(I),I=1,12)
482  4924 FORMAT (1H035X18HINITIAL CONDITIONS// (I5,E10.4,I5,E10.4,I5,
483      1E10.4,I5,E10.4,I5,E10.4,I5,E10.4))
484      CG = COS(QGAM)
485      SG = SIN(QGAM)
486  C
487  C      PART III
488  C
489      IPART = 3
490      CAPM = 0.0
491      DO 3299 I=1,N
492  3299 CAPM = CAPM+EM(I) _____ Total mass.
493      ENZ = SQRT(FMU)/AZ**1.5
494      PZ = AZ*(1.0-EZ**2) _____ Used in Eq. A-46.
495      WZ = WZ*PI/180.
496      EYZ = EYZ*PI/180.
497      THZ = THZ*PI/180.
498      TO = 2.0*PI/ENZ
499      CAPT = TO*ORBS _____ Duration of run (seconds).
500      XIF = SIN(EYZ)
501      XIC = COS(EYZ)
502      THF = SIN(THZ)
503      THC = COS(THZ)
504      PSIS = 2.*PI*FLOAT(ND-80)/365. _____ Eq. A-50.
505      XIS = 23.5*PI/180.
506      SIGDP(1) = COS(PSIS)
507      SIGDP(2) = COS(XIS)*SIN(PSIS)
508      SIGDP(3) = SIN(XIS)*SIN(PSIS) } _____ Eq. A-51.
509      WRITE (6,974) SIGDP
510  974  FORMAT (1H05X3HSUN7X3E16.7)
511      DO 420 I = 1,NM
512      DO 410 J = 1,NM
513      PSQ(I,J) = S(I+1,J)
514  410  PQ(I,J) = 0.
515  420  PQ(I,I) = 1.

```

NOTE Background for remainder of Part III is contained in Ref. 3.

```

516      MQ = 25
517      LQ = XSIMEQ(MQ,NM,NM,PSQ,PQ,DQ,JQ) ----- Theorem 2 of Ref. 3.
518      GO TO (425,900,910),LQ
519 425   DO 440 I = 1,N3
520      Z(I,1) = 0.
521      DO 430 J = 1,NM
522      Z(I,J+1) = 0.
523      DO 430 K = 1,NM
524 430   Z(I,J+1) = Z(I,J+1)+C(I,K)*PSQ(K,J) ----- Matrix [D] of Ref. 3. NOTE: Original [C]
525      DO 440 J = 1,N                               is no longer needed; its storage can now be used
526      C(I,J) = 0.                                   for other computations.
527      DO 440 K = 1,N
528      DUM = -EM(K)/CAPM
529      IF(K.EQ.J) DUM = DUM+1.
530 440   C(I,J) = C(I,J)+Z(I,K)*DUM*EM(J) ----- Product [D][μ] of Ref. 3.
531      DO 450 I=1,N3
532      DO 450 J = 1,N3
533      PSI(I,J) = 0.
534      DO 450 K = 1,N
535 450   PSI(I,J) = PSI(I,J)+C(I,K)*Z(J,K) ----- Matrix [J] of Ref. 3.
536      WRITE (6,17249)
537 17249  FORMAT (1H )
538      DO 4705 I=1,N3
539      IALF = 1+MOD(I-1,3)
540      ICAP = 1+(I-IALF)/3
541      DO 470 J=1,N3
542      IBET = 1+MOD(J-1,3)
543      JCAP = 1+(J-IBET)/3
544      IF (ICAP-JCAP) 470,3701,470
545 3701  CONTINUE
546      TAU = 0.
547      IF (IALF-IBET) 4702,4703,4702
548 4703  CONTINUE
549      IF(IALF.EQ.IBET) TAU =
550      1PSI(3*ICAP,3*ICAP)+PSI(3*ICAP-1,3*ICAP-1)+PSI(3*ICAP-2,3*ICAP-2)
551 4702  CONTINUE
552      TAU = TAU-PSI(I,J)
553      A(ICAP,IALF,IBET) = A(ICAP,IALF,IBET)+TAU ----- Constant augmented inertia matrix.
554 470   CONTINUE
555 4705  CONTINUE
556      DO 480 I = 1,N3
557      IALF = 1+MOD(I-1,3)
558      ICAP = 1+(I-IALF)/3

```

```

559      DO 480 J=1,N
560      PSI(I,J) = 0.
561      DO 475 K=1,N
562 475    PSI(I,J) = PSI(I,J)+Z(I,K)*FM(K)
563      PSI(I,J)=-PSI(I,J)/CAPM+Z(I,J)
564 480    CONTINUE
565      DO 490 I = 1,N3
566      IALF = 1+MOD(I-1,3)
567      ICAP = 1+(I-IALF)/3
568      DO 490 J=1,N
569 490    B(ICAP,J,IALF) = PSI(I,J) _____ Barycentric vectors.
570  C
571  C      PART IV
572  C
573      DO 495 I=1,N
574      DO 495 L=1,3
575      II = N3+(I-1)*9+(L-1)*3
576      DO 495 K=1,3
577 495    Y(II+K) = TH(I,K,L)
578      TR = T0/ENR
579      LICE = 4
580      NV = 12*N
581      T = 0.0
582      GO TO 831
583 800    CALL ICE (TR,T,TP,NV,Y,DY,DICE,LICE,IND,IORD,KPRI,ERL) _____ Numerical integration.
584      GO TO (810,820,830,840),LICE
585  C      BOX A
586 810    DO 500 I = 1,N
587      II = N3+(I-1)*9
588      DO 500 K = 1,3
589      DO 500 L = 1,3
590 500    TH(I,K,L) = Y(II+3*L-3+K)
591      KRUM = KRUM+1
592      IPART = 4
593      AM = ENZ*(T-TZ)
594      COAM = COS(AM)
595      RS = AZ*(1.-EZ*(COAM+.5*EZ*(COS(AM+AM)-1.+ .75*EZ*(COS(3.*AM)-COAM)
596 1))) _____ Eq. A-49.
597      SCRf = 2.0*(1.0-SQRT(1.0-(ERRD/RS)**2)) _____ Eq. A-14.
598      RMU = 3.*FMU*RS**(-3)
599      VV = AM+2.0*EZ*SIN(AM)+1.25*EZ**2*SIN(2.0*AM)
600 1+1.0/12.0*EZ**3*(13.0*SIN(3.0*AM)-3.0*SIN(AM)) _____ Eq. A-52.
601      CV = COS(VV)

```

Preparation for numerical integration.

```

602 SV = SIN(VV)
603 SWZ = SIN(WZ)
604 CWZ = COS(WZ)
605 VC = CWZ*CV-SWZ*SV
606 VF = SWZ*CV+CWZ*SV
607 SIGP(1) = (-THC*VF-THF*XIC*VC)*SIGDP(1)+(-THF*VF+THC*XIC*VC)
608 1*SIGDP(2)+XIF*VC*SIGDP(3)
609 SIGP(2) = THF*XIF*SIGDP(1)-THC*XIF*SIGDP(2)+XIC*SIGDP(3)
610 D13 = THC*VC-THF*XIC*VF
611 D23 = THF*VC+THC*XIC*VF
612 D33 = XIF*VF
613 SIGP(3) = D13*SIGDP(1)+D23*SIGDP(2)+D33*SIGDP(3)
614 DO 530 I = 1,N
615 ICON = 3*(I-1)
616 DO 510 J = 1,3
617 U(J) = 0.
618 DO 510 K = 1,3
619 510 U(J) = U(J)+A(I,J,K)*WM(K,I)
620 UU(ICON+1) = WM(2,I)*U(3)-WM(3,I)*U(2)
621 UU(ICON+2) = WM(3,I)*U(1)-WM(1,I)*U(3)
622 UU(ICON+3) = WM(1,I)*U(2)-WM(2,I)*U(1)
623 DO 520 J = 1,3
624 U(J) = 0.
625 DO 520 K = 1,3
626 520 U(J) = U(J)+A(I,J,K)*TH(I,3,K) _____ First term of Eq. 19 of Ref. 3.
627 H(ICON+1) = RMU*(TH(I,3,2)*U(3)-TH(I,3,3)*U(2))
628 H(ICON+2) = RMU*(TH(I,3,3)*U(1)-TH(I,3,1)*U(3))
629 530 H(ICON+3) = RMU*(TH(I,3,1)*U(2)-TH(I,3,2)*U(1))
630 DO 550 I = 1,N3
631 EL(I) = 0.
632 Q(I) = 0.
633 G(I) = 0.
634 DO 550 J = 1,N3
635 550 PSI(I,J) = 0.
636 RUM = FMU*CAPM*RS**(-3)
637 DUM = -SQRT(1.0-(ERRD/RS)**2)
638 IS = 1
639 IF(SIGP(3).GT.DUM) IS = 2 _____ In sunlight.
640 DO 730 I = 1,N
641 IF (IS .EQ. 1 ) GO TO 140
642 141 DO 143 JJ = 1,3
643 SIG(JJ,I) = 0.0
644 DO 143 K = 1,3

```

```

645 143 SIG(JJ,I) = SIG(JJ,I)+TH(I,K,JJ)*SIGP(K) ----- Eq. A-54.
646     IF(I.NE.1) GO TO 144
647     DO 145 JJ = 1,3
648 145 UP(JJ) = -SIG(JJ,I)*2.0*SPC*AE(1) ----- Solar pressure force on sphere.
649     GO TO 140
650 144 UP(1) = 0.0
651     DO 146 JJ = 2,3
652 146 UP(JJ) = -SIG(JJ,I)*2.0*SPC*SQRT(SIG(2,I)**2+SIG(3,I)**2)*AE(I) ----- Solar pressure force
653 140 CONTINUE                                     on cylinder.
654     ICON = 3*(I-1)
655     DO 730 J = 1,N
656     JCON = 3*(J-1)
657     DO 670 JJ = 1,3
658     DO 660 II = 1,3
659     V(II,JJ) = 0.
660     DO 660 K = 1,3
661 660 V(II,JJ) = V(II,JJ)+TH(I,K,II)*TH(J,K,JJ)
662     P(1,JJ) = B(I,J,2)*V(3,JJ)-B(I,J,3)*V(2,JJ)
663     P(2,JJ) = B(I,J,3)*V(1,JJ)-B(I,J,1)*V(3,JJ)
664 670 P(3,JJ) = B(I,J,1)*V(2,JJ)-B(I,J,2)*V(1,JJ) } ----- Eq. 12b of Ref. 3.
665     DO 690 K = 1,3
666     II = ICON+K
667     IF(I.EQ.J) GO TO 680
668     PSI(II,JCON+1) = CAPM*(P(K,2)*B(J,I,3)-P(K,3)*B(J,I,2))
669     PSI(II,JCON+2) = CAPM*(P(K,3)*B(J,I,1)-P(K,1)*B(J,I,3))
670     PSI(II,JCON+3) = CAPM*(P(K,1)*B(J,I,2)-P(K,2)*B(J,I,1)) } ----- Eq. 14c of Ref. 3;
671     GO TO 690                                     applicable for I ≠ J.
672 680 PSI(II,JCON+1) = A(I,K,1)
673     PSI(II,JCON+2) = A(I,K,2)
674     PSI(II,JCON+3) = A(I,K,3)
675 690 CONTINUE
676     DO 700 K = 1,3
677     U(K) = 0.
678     DO 700 L = 1,3
679     DUM = 3.*TH(J,3,K)*TH(J,3,L)
680     IF(K.EQ.L) DUM = DUM-1.
681 700 U(K) = U(K)+DUM*B(J,I,L)
682     IF (I .EQ. J) GO TO 7210
683     DO 710 K = 1,3
684 710 G(ICON+K) = G(ICON+K)+RUM*(P(K,1)*U(1)+P(K,2)*U(2)+P(K,3)*U(3)) ----- Second term of Eq. 19
685     U(1) = -B(J,I,1)*(WM(3,J)**2+WM(2,J)**2)+B(J,I,2)* of Ref. 3.
686     1WM(1,J)*WM(2,J)+B(J,I,3)*WM(1,J)*WM(3,J)
687     U(2) = B(J,I,1)*WM(1,J)*WM(2,J)-B(J,I,2)*(WM(1,J)**2+

```

```

688      1WM(3,J)**2)+B(J,I,3)*WM(2,J)*WM(3,J)
689      U(3) = B(J,I,1)*WM(1,J)*WM(3,J)+B(J,I,2)*WM(2,J)*WM(3,J)
690      1-B(J,I,3)*(WM(1,J)**2+WM(2,J)**2)
691      DO 720 K = 1,3
692      720 Q(ICON+K) = Q(ICON+K)+CAPM*(P(K,1)*U(1)+P(K,2)*U(2)+P(K,3)*U(3)) —— Eq. 14d of Ref. 3.
693      7210 CONTINUE
694      GO TO (147,148),IS
695      148 DO 149 JJ = 1,3
696      K = 3*(I-1)+JJ
697      149 G(K) = G(K)+P(JJ,1)*UP(1)+P(JJ,2)*UP(2)+P(JJ,3)*UP(3) —— Add moment of solar
698      147 CONTINUE                                     pressure force.
699      730 CONTINUE
700      DO 650 I = 1,N
701      ICON = 3*(I-1)
702      DO 6500 J=1,NM
703      IF (S(I,J)-1.0) 6500,735,6500
704      735 KAY = 0
705      DO 560 K = 1,N
706      IF(K.EQ.I) GO TO 560
707      IF(S(K,J)) 555,560,555
708      555 IF(KAY.NE.0) GO TO 920
709      KAY = K
710      560 CONTINUE
711      IF(KAY.LE.0) GO TO 920
712      IF(S(KAY,J)+1.) 920,565,920
713      565 TRACE = 0.
714      ZIS = IS
715      DO 150 II = 1,3
716      150 DELT(II) = 0.0 —— No thermal effects at damper hinge.
717      IF(J.EQ.1) GO TO 151
718      DELT(2) = -SCRF*XJE*TH(I,3,3)+XJS*(SIG(3,I)-0.4*SCRF*TH(I,3,3))*
719      1(ZIS-1.0) —— Eq. A-18.
720      DELT(3) = -SCRF*XJE*TH(I,3,2)+XJS*(SIG(2,I)-0.4*SCRF*TH(I,3,2))*
721      1(ZIS-1.0) —— Eq. A-20.
722      IF (J .EQ. 1 .OR. J .GT. 5) GO TO 151
723      DELT(2) = DELT(2)/2.
724      DELT(3) = DELT(3)/2.
725      151 CONTINUE
726      YYY = DELT(2)
727      ZZZ = DELT(3)
728      YYS = YYY**2
729      ZZS = ZZZ**2
730      SQUR = SQRT(1.0-YYS-ZZS)

```

Location of adjacent members for internal torques.

See discussion at beginning of Appendix C.



```

731     DDRD(1,1) = SQUR
732     DDRD(1,2) = -ZZZ
733     DDRD(1,3) = -YYY
734     DDRD(2,1) = ZZZ
735     DDRD(2,2) = (YYS+ZZS*SQUR)/(YYS+ZZS)
736     DDRD(2,3) = YYY*ZZZ*(SQUR-1.0)/(YYS+ZZS)
737     DDRD(3,1) = YYY
738     DDRD(3,2) = DDRD(2,3)
739     DDRD(3,3) = (ZZS+YYS*SQUR)/(YYS+ZZS)
740     IF (YYS+ZZS .LT. 1.E-30) DDRD(2,2) = 1.0
741     IF (YYS+ZZS .LT. 1.E-30) DDRD(3,3) = 1.0
742     DO 11119 II=1,3
743     DO 11119 JJ=1,3
744     RHOP(J,II,JJ) = 0.0
745     DO 11119 KK=1,3
746 11119 RHOP(J,II,JJ) = RHOP(J,II,JJ)+DDRD(II,KK)*RHO(J,KK,JJ)
747 152 CONTINUE
748     DO 570 K = 1,3
749     DO 570 L = 1,3
750     VP(K,L) = 0.
751     DO 570 JJ = 1,3
752 570 VP(K,L) = VP(K,L)+TH(I,JJ,K)*TH(KAY,JJ,L)
753     DO 590 K = 1,3
754     DO 580 L = 1,3
755     V(K,L) = 0.
756     DO 580 II = 1,3
757 580 V(K,L) = V(K,L)+VP(L,II)*RHOP(J,K,II)
758 590 TRACE = TRACE+V(K,K)
759     IF (ABS(V(1,2))+ABS(V(1,3))+ABS(V(2,3)) .LT. .01) GO TO 603
760     CAMB = .5*(TRACE-1.)
761     IF(ABS(CAMB).LT.1.) GO TO 595
762     CAMB = SIGN(1.,CAMB)
763 595 AMBDA = ACOS(CAMB)
764 C     EIGENVECTOR OF V/
765     IF(ABS(V(2,3)).GT.ABS(V(1,2))) GO TO 596
766     IF(ABS(V(1,3)).GT.ABS(V(1,2))) GO TO 597
767     U(1) = V(1,2)*V(2,3)-V(1,3)*(V(2,2)-1.)
768     U(2) = V(1,3)*V(2,1)-V(2,3)*(V(1,1)-1.)
769     U(3) = (V(1,1)-1.)*(V(2,2)-1.)-V(1,2)*V(2,1)
770     GO TO 599
771 596 IF(ABS(V(2,3)).GT.ABS(V(1,3))) GO TO 598
772 597 U(1) = V(3,2)*V(1,3)-V(1,2)*(V(3,3)-1.)
773     U(2) = (V(1,1)-1.)*(V(3,3)-1.)-V(1,3)*V(3,1)

```

} Eq. A-21.

} Elimination of possible indeterminacy in Eq. A-21.

\_\_\_\_\_ Eqs. A-9 and A-21.

\_\_\_\_\_ Eq. A-1.

\_\_\_\_\_ Off-diagonal vector element for small angles.

\_\_\_\_\_ Overrides small numerical error.

\_\_\_\_\_ Eq. A-2.

\_\_\_\_\_ See Eq. A-3.

} Cross product of 1st and 2nd rows of [V-I].

```

774      U(3) = V(3,1)*V(1,2)-V(3,2)*(V(1,1)-1.)
775      GO TO 599
776      598  U(1) = (V(2,2)-1.)*(V(3,3)-1.)-V(2,3)*V(3,2)
777          U(2) = V(2,3)*V(3,1)-V(2,1)*(V(3,3)-1.)
778          U(3) = V(2,1)*V(3,2)-(V(2,2)-1.)*V(3,1)
779      599  UNRM = SQRT(U(1)**2+U(2)**2+U(3)**2)
780          DO 600 K = 1,3
781      600  U(K) = U(K)/UNRM
782          U(1) = SIGN(U(1),V(2,3))
783          U(2) = SIGN(U(2),V(3,1))
784          U(3) = SIGN(U(3),V(1,2))
785          GO TO 607
786      603  AMBDA = SQRT(V(1,2)**2+V(2,3)**2+V(3,1)**2)
787          UI1) = V(2,3)/AMBDA
788          U(2) = V(3,1)/AMBDA
789          U(3) = V(1,2)/AMBDA
790      C
791      607  KDN = 3*(KAY-1)
792          DO 610 K=1,3
793          WKP(K) = 0.
794          DO 610 L=1,3
795      610  WKP(K) = WKP(K)+VP(K,L)*WM(L,KAY) ----- Second half of Eq. A-6.
796          DO 630 K = 1,3
797          UP(K)=0.
798          DUM = 0.
799          IF (FD .GT. 1.E-05) GO TO 4871
800          IF (J .NE. 1 .OR. K .NE. 2) GO TO 4871
801          SAMBDA = SIGN(AMBDA,V(3,1))
802          TRYTH = TRH+SIGN(2.0*TPH*(1.0-EXP(-SIGN*ABS(SAMBDA-AMBDL))),AMDDT) ----- Eq. B-26.
803          THH = SIGN(AMIN1(ABS(TRYTH),TPH),TRYTH) ----- Torque saturation.
804          DO 4872 IJK = 1,3
805      4872  UP(2) = UP(2)+R(J,K,IJK)*U(IJK) ----- Damper spring torque (Rigidity coefficient
806          UP(2) = AMBDA*UP(2)+THH ----- assumed fixed, i.e., no damper stops).
807          WKPS = WKP(2)
808          AMBDS = SAMBDA
809          GO TO 630
810      4871  CONTINUE
811          DO 620 L = 1,3
812          UP(K) = UP(K)+RP(J,K,L)*(WKP(L)-WM(L,1)) ----- Viscous Damping.
813      620  DUM = DUM+R(J,K,L)*U(L) } ----- Damping plus spring torque.
814          UP(K) = UP(K)+AMBDA*DUM }
815      630  EL(ICUN+K) = EL(ICUN+K)+UP(K) ----- Internal torque.
816          DO 640 K = 1,3

```

```

817 640 EL(KON+K) = EL(KON+K)-VP(1,K)*UP(1)-VP(2,K)*UP(2)-VP(3,K)*UP(3) ——— Equal and
818 IF (J.EQ. 1) GO TO 6501 ——— No interactions at damper hinge. opposite torque.
819 DO 5546 II=1,3
820 DO 5546 JJ=1,3
821 5546 DVEC(II,JJ) = AMBDA*TH(I,II,JJ)
822 DO 5547 II=1,3
823 UP(II) = 0.0
824 DO 5547 JJ=1,3
825 5547 UP(II) = UP(II)+DVEC(II,JJ)*U(JJ)
826 JS = 1+(J-2)/4
827 DO 5550 II=1,3
828 DVEC(1,II) = 0.0
829 DO 5550 JJ=1,3
830 5550 DVEC(1,II) = DVEC(1,II)+EPSIL(JS,1)*TH(1,JJ,II)*UP(JJ)
831 DO 15551 II=1,3
832 DVEC(2,II) = 0.0
833 DO 5551 JJ=1,3
834 5551 DVEC(2,II) = DVEC(2,II)+DUR(II,JJ)*DVEC(1,JJ)
835 15551 EL(II) = EL(II)+DVEC(2,II)
836 IQ = MOD(J-2,4)+3
837 NPI = NPB+1
838 DO 5552 IP=2,NPI
839 IA = IQ+4*(IP-2)
840 DO 15553 II=1,3
841 DO 15553 JJ=1,3
842 DVEC(II,JJ) = 0.0
843 DO 15553 KK=1,3
844 15553 DVEC(II,JJ) = DVEC(II,JJ)+DUR(II,KK)*TH(IA,JJ,KK)
845 DO 5553 II=1,3
846 IIA = II+3*(IA-1)
847 DO 5553 IJ = 1,3
848 5553 EL(IIA) = EL(IIA)+EPSIL(JS,IP)*DVEC(II,IJ)*UP(IJ)
849 5552 CONTINUE
850 6501 SD(J+1,1) = AMBDA*U(1) ——— Torsional displacement readout.
851 DO 4601 K = 1,3
852 KK = 3*(I-1)+K
853 KL = 3*(J-1)+K
854 IF (MI(KL).EQ. 0) GO TO 4601 ——— Mode not locked.
855 INDX = MI(KL)
856 SQU(KK,INDX) = 1.0
857 DO 4602 IB = 1,3
858 III = 3*(KAY-1)+IB
859 4602 SQU(III,INDX) = -VP(K,IB)

```

See pages 38-40.

Eq. A-28.

```

860      GO TO (4603,4604,4605),K
861      4603 GAM(INDX) = WM(2,I)*WKP(3)-WM(3,I)*WKP(2)
862      GO TO 4601
863      4604 GAM(INDX) = WM(3,I)*WKP(1)-WM(1,I)*WKP(3)
864      GO TO 4601
865      4605 GAM(INDX) = WM(1,I)*WKP(2)-WM(2,I)*WKP(1)
866      4601 CONTINUE
867      6500 CONTINUE
868      650 CONTINUE
869      DO 750 J = 1,N3
870      750 VECT(J) = -UU(J)+H(J)+EL(J)-G(J)+Q(J)
871      DO 5601 I=1,N3
872      DO 5601 J=1,N3
873      5601 PSIV(I,J) = PSI(I,J)
874      7249 FORMAT (1H0/19E11.4)
875      CALL INVERT (PSIV,N3,78)
876      IF (NC .EQ. 0) GO TO 14717
877      DO 4639II = 1,NC
878      DO 4639JJ = 1,NC
879      4639 XT(II,JJ) = 0.0
880      DO 4700 II = 1,N3
881      DO 4700 KK = 1,NC
882      SUM = 0.0
883      DO 4701 LL = 1,N3
884      4701 SUM = SUM+PSIV(II,LL)*SQU(LL,KK)
885      DO 4700 JJ = 1,NC
886      4700 XT(JJ,KK)= XT(JJ,KK)+SQU(II,JJ)*SUM
887      CALL INVERT (XT,NC,38)
888      DO 4712 I = 1,N3
889      XID (I) = 0.0
890      DO 4712 J = 1,N3
891      4712 XID(I) = XID(I)+PSIV(I,J)*VECT(J)
892      DO 4713 I=1,NC
893      XIB(I) = 0.0
894      DO 4713 J = 1,N3
895      4713 XIB(I)=XIB(I)+SQU(J,I)*XID(J)
896      DO 4714 I = 1,NC
897      XID(I) = 0.0
898      DO 4714 J = 1,NC
899      4714 XID(I) = XID(I)+XT(I,J)*XIB(J)
900      DO 4715 I = 1,N3
901      DO 4715 J = 1,NC
902      4715 VECT (I) = VECT(I)-SQU(I,J)*XID(J)

```

} ——— Eq. A-29.

————— Eq. 7, page 9.

————— Matrix  $[F]^T [r]^{-1} [F]$  , Eq. A-31.

————— Vector  $[F]^T [r]^{-1} E$  , Eq. A-31.

```

903      DO 4716 I = 1,NC
904      XID(I) = 0.0
905      DO 4716 J = 1,NC
906 4716  XID(I) = XID(I)+XT(I,J)*GAM(J)
907      DO 4717 I = 1,N3
908      DO 4717 J = 1,NC
909 4717  VECT(I) = VECT(I)-SQU(I,J)*XID(J)
910 14717 CONTINUE
911      DO 5610 I = 1,N3
912      WD(I) = 0.0
913      DO 5610 J = 1,N3
914 5610  WD(I) = WD(I)+VECT(J)*PSIV(I,J) _____  $\dot{\omega}$  from Eq. A-31.
915      CONS = SQRT(FMU*PZ)/RS**2 _____ Eq. A-46.
916      DO 780 I = 1,N
917      II = N3+(I-1)*9
918      DO 780 K = 1,3
919      CONK = (K-2)*CONS
920      DY(II+K) = TH(I,K,2)*WM(3,I)-TH(I,K,3)*WM(2,I)+CONK*TH(I,4-K,1)
921      DY(II+K+3) = TH(I,K,3)*WM(1,I)-TH(I,K,1)*WM(3,I)+CONK*TH(I,4-K,2)
922 780    DY(II+K+6) = TH(I,K,1)*WM(2,I)-TH(I,K,2)*WM(1,I)+CONK*TH(I,4-K,3) } _____ Eq. A-48.
923      IF (IBUG.NE.0) WRITE (6,2060) T,RS,CONS
924      IF (IBUG.NE.0) WRITE (6,2200) (I,UU(I),H(I),EL(I),G(I),Q(I),WV(I), Extra readouts
925      1 WD(I),I=1,N3)
926 2060  FORMAT(1H0/10X16HPART V - TIME = F8.2,19H, ORBITAL RADIUS = Y
927      1 F7.3,17H, ORBITAL RATE = E8.3//)
928 2200  FORMAT(1H0,20X1HW,11X1HH,11X1HL,11X1HG,11X1HQ,7X5HOMEGA,
929      1 3X9HOMEGA DOT//(I10,7E12.4))
930      IF (IBUG.NE.0 .AND. FD .LT. 1.E-05) WRITE (6,7654) AMBDS,AMBDL,
931      1 TRH,TRYTH,THH,AMDDT,WKPS,TPH
932 7654  FORMAT (1H05E18.5)
933      GO TO 800
934 820   CONTINUE
935      KBBC = KBBC+1
936      IF (FD .GT. 1.E-05) GO TO 800
937      AMDDT = WKPS-WM(2,2) _____ Time derivative of damper angle -- See card No. 807.
938      SNN = SIGN(1.0,AMDDT)
939      IF (ABS(SNN+S00) .GT. 1.5) GO TO 4887 _____ denotes no polarity change in hysteresis
940      TRH = THH } _____ Reset values for Eq. B-26.
941      AMBDR = AMBDS }
942 4887  S00 = SNN
943      GO TO 800
944 830   CONTINUE
945      THOUR = T/3600.

```

```

946 WRITE (6,950) THOUR,D13,D23,D33,SHAD(IS)
947 831 DVEC(1,1) = TH(1,1,1)*CG+TH(1,1,2)*SG
948 DVEC(1,2) = -TH(1,1,1)*SG+TH(1,1,2)*CG
949 DVEC(1,3) = TH(1,1,3)
950 DVEC(2,1) = TH(1,2,1)*CG+TH(1,2,2)*SG
951 DVEC(2,2) = -TH(1,2,1)*SG+TH(1,2,2)*CG
952 DVEC(2,3) = TH(1,2,3)
953 DVEC(3,1) = TH(1,3,1)*CG+TH(1,3,2)*SG
954 DVEC(3,2) = -TH(1,3,1)*SG+TH(1,3,2)*CG
955 DVEC(3,3) = TH(1,3,3)

```

Eq. B-27.

```

956 WRITE(6,951){(DVEC(I,J),J = 1,3),I = 1,3}
957 951 FORMAT (1H04OX8HATTITUDE //(20X3E16.7))
958 DO 160 I = 1,3
959 DO 160 J = 1,3
960 DVEC(I,J) = 0.0
961 DO 160 K = 1,3
962 160 DVEC(I,J) = TH(1,K,I)*TH(2,K,J)+DVEC(I,J)
963 DO 161 I = 1,3
964 DO 161 J = 1,3
965 V(I,J) = 0.0
966 DO 161 K = 1,3

```

Eq. B-28.

```

967 161 V(I,J) = V(I,J)+RHO(1,I,K)*DVEC(K,J)
968 WRITE (6,952) V(2,3),V(3,1),V(1,2)
969 952 FORMAT (1H010X6HDAMPER5X3E16.7)
970 DO 162 II = 3,6
971 DO 163 I = 1,3
972 DO 163 J = 1,3
973 DVEC(I,J) = 0.0
974 DO 163 K = 1,3
975 163 DVEC(I,J) = DVEC(I,J)+RHO(II-1,I,K)*TH(1,J,K)
976 DO 164 I = 2,3
977 SD(II,I) = 0.0
978 DO 164 J = 1,3
979 164 SD(II,I) = SD(II,I)+SL*DVEC(I,J)*TH(II,J,1)
980 162 CONTINUE
981 DO 166 K=1,4
982 DO 167 II = 1,3
983 DO 167 JJ = 1,3
984 DVEC(II,JJ) = 0.0
985 DO 167 KK = 1,3
986 167 DVEC(II,JJ) = DVEC(II,JJ)+SL*RHO(K+1,II,KK)* TH(1,JJ,KK)
987 DO 165 J=2,NPB
988 INDX = 4*J+K-2

```

Eq. B-29.

```

989      DO 168 II=2,3
990      SD(INDX,II) = 0.0
991      DO 168 JJ=1,3
992 168   SD(INDX,II) = SD(INDX,II)+DVEC(II,JJ)*TH(INDX,JJ,1)
993 165   CONTINUE
994 166   CONTINUE
995      DO 169 II=2,3
996      DO 169 JJ=7,N
997 169   SD(JJ,II) = SD(JJ,II)+SD(JJ-4,II)
998      WRITE (6,953) (SD(I,3),I = 3,N)
999      WRITE (6,954)(SD(I,2),I = 3,N)
1000     WRITE (6,955)(SD(I,1),I = 3,N)
1001 953   FORMAT (1H030X11HDEFORMATION/4X8HIN PLANE /(15X4E16.7))
1002 954   FORMAT (4X12HOUT OF PLANE /(15X4E16.7))
1003     DO 3330 I = 1,4
1004     J = 4*NPB-2+I
1005     ZIN(I)=SD(J,3)
1006 3330  YIN(I) = SD(J,2)
1007     XINIT(5) = -0.5*(YIN(3)+YIN(4)-YIN(1)-YIN(2))
1008     XINIT(6) = -0.5*(ZIN(3)+ZIN(4)+ZIN(1)+ZIN(2))
1009     XINIT(7) = -0.5*(YIN(3)-YIN(4)-YIN(1)+YIN(2))-2.0*QBA
1010     XINIT(8) = -0.5*(ZIN(3)-ZIN(4)+ZIN(1)-ZIN(2))-2.0*QKA
1011     XINIT(9) = -0.5*(ZIN(3)+ZIN(4)-ZIN(1)-ZIN(2))
1012     XINIT(10) = -0.5*(YIN(3)+YIN(4)+YIN(1)+YIN(2))
1013     XINIT(11) = -0.5*(ZIN(3)-ZIN(4)-ZIN(1)+ZIN(2))
1014     XINIT(12) = -0.5*(YIN(3)-YIN(4)+YIN(1)-YIN(2))
1015     WRITE (6,9511) XINIT(5),XINIT(6),XINIT(7),XINIT(9),XINIT(10),
1016     1XINIT(11),XINIT(8),XINIT(12)
1017 9511  FORMAT (1H027X15HSATELLITE MODES//4X4HROLL9XE10.4,5X5HPITCH
1018     18XE10.4,5X3HYAW10XE10.4//4X12HLONGITUDINAL1XE10.4,5X7HLATERAL
1019     26XE10.4,5X8HVERTICAL5XE10.4//4X16HIN PLANE NEUTRAL5XE10.4,
1020     36X20HOUT OF PLANE NEUTRAL6XE10.4)
1021     IF (T .GT. CAPT) GO TO 9999
1022     TP = T+TR
1023     GO TO 800
1024 840   CONTINUE
1025     GO TO 800
1026 2080  FORMAT(1H1,30X36HBEGIN INTEGRATION, PRINT INTERVAL =F8.4//)
1027 C     ERROR STOPS
1028 900   WRITE(6,3100) IPART
1029     GO TO 990
1030 910   WRITE(6,3110) IPART
1031     GO TO 990

```

} — Eq. B-29.

————— Eq. B-31.

————— Duration of program run.

```
1032 920 WRITE(6,3120)(S(K,J),K=1,N)
1033 990 WRITE(6,3000)
1034 999 GO TO 9999
1035 950 FORMAT (1H15X4HT = E16.7,6H HOURS5X9HSATELLITE3X3E16.7,4XA6)
1036 955 FORMAT (4X5HTWIST /(15X4E16.7))
1037 3000 FORMAT(1H0,15X,18H*** ERROR STOP ***)
1038 3100 FORMAT(1H0,10X14HOVERFLOW, PART 13)
1039 3110 FORMAT(1H0,10X,21HSINGULAR MATRIX, PART 13)
1040 3120 FORMAT(1H0,10X,24HBAD COLUMN IN MATRIX /S///(15F6.1))
1041 END
```



## Subroutines

Following are listings for standard Westinghouse subroutines ICE, INTEG, INVERT, and XSIMEQ. For theoretical descriptions of these computational schemes the reader is referred to "Standard Subroutines Used by Westinghouse RAE Operational Programs," April, 1968, Contract No. NAS5-9753-20.

1		SUBROUTINE ICE (P,TT,TP,NN,Y,DY,F,L,INDEX,I,KPRI,ERL)	
2		DIMENSION ERL(1)	
3		DIMENSION DUMPR(312)	
4		DIMENSION Y(1),DY(1),F(1)	AAIC0030
5	C	DIMENSION Y(1),DY(1),F(1)	AAIC0040
6		T = TT	AAIC0050
7		GO TO (100,200,300,400),L	AAIC0060
8	100	IG=IG	AAIC0070
9		GO TO (101,102),IG	AAIC0080
10	101	J = 1	AAIC0090
11		L = 2	AAIC0100
12		M = 0	AAIC0110
13		TS = T	AAIC0120
14		DO 106 K = 1,N	AAIC0130
15		K1 = K+3*N	AAIC0140
16		K2 = K1+N	AAIC0150
17		K3 = N + K	AAIC0160
18		F(K1) = Y(K)	AAIC0170
19		F(K3) = F(K1)	AAIC0180
20	106	F(K2) = DY(K)	AAIC0190
21		GO TO 402	AAIC0200
22	102	CALL INTEG(T,DT, N,Y(1),DY(1),F(1),J,I)	AAIC0210
23		J = J+1	AAIC0220
24		IF(J-I ) 103,103,104	AAIC0230
25	103	L = 1	AAIC0240
26		GO TO 402	AAIC0250
27	104	M = M+1	AAIC0260
28	105	GO TO (110,120,130),M	AAIC0270
29	110	DO 111 K = 1,N	AAIC0280
30		K1 = K+N+N	AAIC0290
31	111	F(K1) = Y(K)	AAIC0300
32	112	DO 113 K = 1,N	AAIC0310
33		K1 = K+3*N	AAIC0320
34		K2 = K1+N	AAIC0330
35		K3 = N + K	AAIC0340
36		Y(K) = F(K1)	AAIC0350
37		F(K3) = F(K1)	AAIC0360
38	113	DY(K) = F(K2)	
39			
40		T = TS	AAIC0380
41		IF(T) 114,116,114	AAIC0390
42	114	IF(ABS(H/T)-.000001) 115,115,116	AAIC0400

43	115	M = 0	AAIC0410
44		L = 4	AAIC0420
45		GO TO 402	AAIC0430
46	116	DT = .5*H	AAIC0440
47		M = 1	AAIC0450
48		J = 1	AAIC0460
49		GO TO 300	AAIC0470
50	120	DO 121 K = 1,N	AAIC0480
51		K1 = K+N	AAIC0490
52	121	F(K1) = Y(K)	AAIC0500
53		M = 2	AAIC0510
54		J = 1	AAIC0520
55		IG = 2	AAIC0530
56		L = 1	AAIC0540
57		GO TO 402	AAIC0550
58	130	DO 131 K = 1,N	AAIC0560
59		K1 = K+2*N	AAIC0570
60		F(K) = (Y(K)-F(K1))/(2.0*I-1.0)	AAIC0580
61		DUMPR(K) = Y(K)	
62		Y(K) = Y(K) +F(K)	AAIC0590
63	131	CONTINUE	AAIC0640
64		IF (KPRI .EQ. 0) GO TO 1324	
65		WRITE (6,1325) T	
66	1325	FORMAT (1H15X18HATTEMPTED STEP AT E10.4//10X2HY1,10X2HY210X2HYE10	
67		1X2HER//)	
68		DO 1326 IKZ = 1,N	
69		IAM = 2*N+IKZ	
70	1326	WRITE (6,1327) IKZ,F(IAM),DUMPR(IKZ),Y(IKZ),F(IKZ)	
71	1327	FORMAT (15,4E12.4)	
72	1324	CONTINUE	
73		DO 1967 K=1,N	
74		IF (ABS(F(K)) .GT. ABS(ERL(K))/20.) GO TO 135	
75	1967	CONTINUE	
76	134	H = H+H	AAIC0740
77	1345	DT = H	AAIC0750
78		GO TO 401	AAIC0760
79	135	DO 1968 K=1,N	
80		IF (ABS(F(K)) .GT. ABS(ERL(K))) GO TO 136	
81	1968	CONTINUE	
82		GO TO 1345	
83	136	DO 137 K = 1,N	AAIC0780
84		K1 = K+N	AAIC0790
85		K2 = K+N+N	AAIC0800

86	137	F(K2) = F(K1)	AAIC0810
87	138	H = .5*H	AAIC0820
88		MU=2	
89		GO TO 112	AAIC0830
90	200	MU=MU	AAIC0840
91		GO TO (203,204),MU	AAIC0850
92	203	H= AMAX1(AMAX1(H,H1),H2)	AAIC0860
93		MU = 2	AAIC0870
94	204	H1 = ABS(H)	AAIC0880
95		IF(P) 205,206,206	AAIC0890
96	205	H = -H1	AAIC0900
97		GO TO 207	AAIC0910
98	206	H = H1	AAIC0920
99	207	IF(ABS(P)-H1) 208,209,209	AAIC0930
100	208	H = P	AAIC0940
101	209	T2 = TP-T	AAIC0950
102		IF(T2) 210,212,210	AAIC0960
103	210	H2 = ABS(T2)	AAIC0970
104		IF(TP) 211,213,211	AAIC0980
105	211	IF(ABS(T2/TP)-.00001) 212,213,213	AAIC0990
106	212	T = TP	AAIC1000
107		DT = H	AAIC1010
108		L = 3	AAIC1020
109		GO TO 402	AAIC1030
110	213	M = 0	AAIC1040
111		J = 1	AAIC1050
112		IF(H1-H2) 215,215,214	AAIC1060
113	214	MU = 1	AAIC1070
114		H = T2	AAIC1080
115	215	DT = H	AAIC1090
116	300	IG = 2	AAIC1100
117		GO TO 102	AAIC1110
118	400	MU = 2	AAIC1120
119		H = P	AAIC1130
120		DT = P	AAIC1140
121		N = NN	AAIC1150
122	401	IG = 1	AAIC1160
123		L = 1	AAIC1170
124	402	TT = T	AAIC1180
125		RETURN	AAIC1190
126		END	AAIC1200

1	C	ICE INTEGRATION SUBROUTINE	0010
2	C	I = 2 SECOND ORDER RUNGE-KUTTA	0020
3	C	I = 3 THIRD ORDER RUNGE-KUTTA	0030
4	C	I = 4 FOURTH ORDER RUNGE-KUTTA	0040
5	C	STORAGE F1 = E = Z1	0050
6	C	F2 = YHAF1 TEMPORARY STORAGE REQUIRED=	0060
7	C	F3 = YFULL DIMENSION OF F ARRAY =	0070
8	C	F4 = YSAVE N*(3+I)	0080
9	C	F5 = DYSAVE WHERE N = NO OF DERIVATIVES	0090
10	C	F6 = Z2 AND I = ORDER OF INTEGRATION	0100
11	C	F7 = Z3 PROCESS	0110
12		SUBROUTINE INTEG (T,DT, N,Y,DY,F,J,I)	0120
13		DIMENSION Y(1),DY(1),F(1)	0130
14	C	DIMENSION Y(1),DY(1),F(1)	0140
15		DO 100 K = 1,N	0150
16		K1 = K	0160
17		K2 = K+5*N	0170
18		K3 = K2+N	0180
19		K4 = K + N	0190
20		GO TO (999,85,95,95),I	0200
21	85	GO TO (86,2,999,999),J	0210
22	86	F(K1) = DY(K)*DT	0220
23		Y(K) = F(K4) + F(K1)	0230
24		GO TO 100	0240
25	95	GO TO (1,2,3,4),J	0250
26	1	F(K1) = DY(K)*DT	0260
27		Y(K) = F(K4)+.5*F(K1)	0270
28		GO TO 100	0280
29	2	F(K2) = DY(K)*DT	0290
30		GO TO (999,22,23,24),I	0300
31	3	F(K3) = DY(K)*DT	0310
32		GO TO (999,33,33,34),I	0320
33	4	Y(K) = F(K4)+(F(K1)+2.0*(F(K2)+F(K3))+DY(K)*DT)/6.0	0330
34		GO TO 100	0340
35	22	Y(K) = .5*(F(K1)+F(K2))	0350
36		GO TO 25	0360
37	23	Y(K) = 2.0*F(K2)-F(K1)	0370
38		GO TO 25	0380
39	24	Y(K) = .5*F(K2)	0390
40	25	Y(K) = Y(K)+F(K4)	0400
41		GO TO 100	0410
42	33	Y(K) = F(K4)+(F(K1)+4.0*F(K2)+F(K3))/6.0	0420

43		GO TO 100	0430
44	34	Y(K) = F(K4)+F(K3)	0440
45	100	CONTINUE	0450
46		GO TO (110,120,130,140),J	0460
47	110	GO TO (999,131,132,132),I	0470
48	120	GO TO (999,140,132,140),I	0480
49	130	GO TO (999,140,140,132),I	0490
50	131	T = DT + T	0500
51		GO TO 140	0510
52	132	T = T + .5*DT	0520
53	140	RETURN	0530
54	999	PAUSE	0540
55		GO TO 140	0550
56		END	0560

```

1  C      MATRIX INVERSION BY GAUSS-JORDAN ELIMINATION
2      SUBROUTINE INVERT(A,N,NN)
3      DIMENSION A(NN,N),B(350),C(350),LZ(350)
4      IF ( N.EQ.1) GO TO 300
5      SUM=1.
6      DO 5 I=1,N
7      5   SUM=SUM*A(I,I)
8  C
9      RAVG=10.**(-ALOG10(SUM)/N)
10 C
11     DO 6 I=1,N
12     DO 6 J=1,N
13     6   A(I,J)=A(I,J)*RAVG
14 C
15     DO 10 J = 1,N
16     10  LZ(J) = J
17     DO 20 I = 1,N
18     K = I
19     Y = A(I,I)
20     L = I-1
21     LP = I+1
22     IF(N-LP) 14,11,11
23     11  DO 13 J = LP,N
24     W = A(I,J)
25     IF(ABS(W)-ABS(Y)) 13,13,12
26     12  K = J
27     Y = W
28     13  CONTINUE
29     14  IF(Y.LT.1.E-8) GO TO 260
30     DO 15 J = 1,N
31     C(J) = A(J,K)
32     A(J,K) = A(J,I)
33     A(J,I) = -C(J)/Y
34     A(I,J) = A(I,J)/Y
35     15  B(J) = A(I,J)
36     A(I,I) = 1./Y
37     J = LZ(I)
38     LZ(I) = LZ(K)
39     LZ(K) = J
40     DO 19 K = 1,N
41     IF(I-K) 16,19,16
42     16  DO 18 J = 1,N

```

```

43      IF(I-J) 17,18,17
44      17  A(K,J) = A(K,J)-B(J)*C(K)
45      18  CONTINUE
46      19  CONTINUE
47      20  CONTINUE
48      DO 200 I = 1,N
49      IF(I-LZ(I)) 100,200,100
50      100  K = I+1
51      DO 500 J = K,N
52      IF(I-LZ(J)) 500,600,500
53      600  M =LZ(I)
54      LZ(I) = LZ(J)
55      LZ(J) = M
56      DO 700 L = 1,N
57      C(L) = A(I,L)
58      A(I,L) = A(J,L)
59      700  A(J,L) = C(L)
60      500  CONTINUE
61      200  CONTINUE
62      C
63      C
64      C      MAKE IT A SYMMETRIC MATRIX
65      C
66      DO 250 I=1,N
67      DO 250 J=I,N
68      AVG=(A(I,J)+A(J,I))/2.*RAVG
69      A(I,J)=AVG
70      A(      J,I)=AVG
71      250  CONTINUE
72      C
73      RETURN
74      300  IF(ABS (A(1,1)).LT.1.E-10 )N=-IABS(N)
75      A(1,1)=1./A(1,1)
76      RETURN
77      C
78      260  N=-IABS(N)
79      RETURN
80      END

```



1		INTEGER FUNCTION XSIMEQ(IMAX,N,M,A,B,DET,IE)	SIME0001
2		DIMENSION A(IMAX,IMAX),B(IMAX,IMAX),IE(IMAX)	SIME0002
3		CALL OVERFL(JO)	
4		CALL D VCHK(JI)	
5		DO 43 I=1,N	SIME0003
6	43	IE(I) = I	SIME0004
7		DO 1 IN = 1,N	SIME0005
8		AMAX = A(IN,IN)	SIME0006
9		II = IN	SIME0007
10		JJ = IN	SIME0008
11		DO 11 I = IN,N	SIME0009
12		DO 11 J = IN,N	SIME0010
13		ZMT = ABS (A(I,J))	SIME0011
14		IF(AMAX-ZMT)10,11,11	SIME0012
15	10	AMAX = ZMT	SIME0013
16		II = I	SIME0014
17		JJ = J	SIME0015
18	11	CONTINUE	SIME0016
19		IF (A(II,JJ)) 69,33,69	SIME0017
20	69	IF(II-IN) 13,17,13	SIME0018
21	13	DO 15 J = 1,N	SIME0019
22		R = A(II,J)	SIME0020
23		A(II,J) = A(IN,J)	SIME0021
24	14	A(IN,J) = R	SIME0022
25		IF(J-M) 19,19,15	SIME0023
26	19	R = B(II,J)	SIME0024
27		B(II,J) = B(IN,J)	SIME0025
28		B(IN,J) = R	SIME0026
29	15	CONTINUE	SIME0027
30	17	IF(JJ-IN) 16,18,16	SIME0028
31	16	DO 24 I = 1,N	SIME0029
32		R = A(I,JJ)	SIME0030
33		A(I,JJ) = A(I,IN)	SIME0031
34	24	A(I,IN) = R	SIME0032
35		IQ=IE(IN)	SIME0033
36		IE(IN)=IE(JJ)	SIME0034
37		IE(JJ) =IQ	SIME0035
38	18	DET = DET*AMAX *(-1.)*((II-IN)+(JJ-IN))	SIME0036
39		KI = IN+1	SIME0037
40		IF (KI-N) 143,143,144	SIME0038
41	143	DO 160 J = 1,M	SIME0039
42		B(IN,J) = B(IN,J)/A(IN,IN)	SIME0040

43		DO 160 K = KI,N	SIME0041
44	160	B(K,J) = B(K,J)-A(K,IN)*B(IN,J)	SIME0042
45		DO 80 J = KI,N	SIME0043
46		A(IN,J) = A(IN,J)/A(IN,IN)	SIME0044
47		DO 80 K = KI,N	SIME0045
48	80	A(K,J) = A(K,J)-A(K,IN)*A(IN,J)	SIME0046
49		DO 1 K = KI,N	SIME0047
50	1	A(K,IN) = 0.	SIME0048
51	145	A(IN,IN) = 1.	SIME0049
52		NF = N-1	SIME0050
53		IF(NF.LE.0)GO TO 147	
54		DO 109 K = 1,NF	SIME0051
55		I = N-K	SIME0052
56		NK = I+1	SIME0053
57		DO 109 L = 1,M	SIME0054
58		SUM = 0.	SIME0055
59		DO 110 J = NK,N	SIME0056
60	110	SUM = SUM+A(I,J)*B(J,L)	SIME0057
61	109	B(I,L) = B(I,L)-SUM	SIME0058
62	147	CONTINUE	
63		DO 111 K = 1,N	SIME0059
64		DO 111 I = 1,N	SIME0060
65		IF(IE(I)-K) 111,113,111	SIME0061
66	111	CONTINUE	SIME0062
67		DO 118 I = 1,N	SIME0063
68		DO 118 J = 1,M	SIME0064
69	118	A(I,J) = B(I,J)	SIME0065
70		CALL OVERFL(JO)	SIME0066
71		CALL D VCHK(JI)	SIME0067
72		GO TO (139,140), JO	SIME0068
73	140	GO TO (139,141),JI	SIME0069
74	141	XSIMEQ = 1	SIME0070
75	189	RETURN	SIME0071
76	33	XSIMEQ = 3	SIME0072
77		GO TO 189	SIME0073
78	144	DO 161 J = 1,M	SIME0074
79	161	B(IN,J) = B(IN,J)/A(IN,IN)	SIME0075
80		GO TO 145	SIME0076
81	139	XSIMEQ = 2	SIME0077
82		GO TO 189	SIME0078
83	113	DO 114 L=1,M	SIME0079
84		Q = B(I,L)	SIME0080
85		B(I,L) = B(K,L)	SIME0081

```
86      114 B(K,L) = Q
87      IQ = IE(K)
88      IE(K) = IE(I)
89      IE(I) = IQ
90      GO TO 111
91      END
```

```
SIME0082
SIME0083
SIME0084
SIME0085
SIME0086
SIME0087
```

## REFERENCES

1. Fletcher, H.J., L. Rongved, and E. Yu, "Dynamics Analysis of a Two-Body Gravitationally Oriented Satellite", *BSTJ* 42, 2239-2266 (1963).
2. Hooker, W. and G. Margulies, "The Dynamical Equations for an n-Body Satellite", *J. Astro. Sci.* XII, 123-128 (Winter, 1965).
3. Roberson, R.E. and J. Wittenburg, "A Dynamical Formalism for an Arbitrary Number of Interconnected Rigid Bodies, with Reference to the Problem of Satellite Attitude Control", IFAC Paper No. 46.D, London, 24 June 1966.
4. Stone, R.G., "RAE -- 1500 Foot Antenna Satellite", *Astronautics and Aeronautics*, March 1965, p. 46.
5. Fixler, S.Z., "Effects of Solar Environment and Aerodynamic Drag on Structural Booms in Space", *AIAA J. Spacecraft and Rockets* 4, 315-321 (1967).
6. Levin, E., "Reflected Radiation Received by an Earth Satellite", *ARSJ* 32, 1328-1331 (1962).
7. Jensen, J. et. al., *Design Guide to Orbital Flight*, New York, McGraw-Hill, 1962, pp. 795 and 842.
8. Blanco, V.M. and S.W. McCuskey, *Basic Physics of the Solar System*, Reading Mass., Addison-Wesley, 1961, p. 53 and 286.
9. Danby, J.M.A., *Fundamental of Celestial Mechanics*, New York, Macmillan, 1964.
10. Tinling, B.E. and V.K. Merrick, "Exploitation of Inertial Coupling in Passive Gravity-Gradient-Stabilized Satellites", *AIAA J. Spacecraft and Rockets* 1, 381-387 (1964).
11. Rimrott, F.P.J., "Storable Tubular Extendible Member", *Machine Design* 37, 28, 156-165 (1965).
12. Newton, J.K. and J.L. Farrell, "Natural Frequencies of a Flexible Gravity Gradient Satellite", to appear in *AIAA Journal of Spacecraft and Rockets*.
13. Wylie, C.R., *Advanced Engineering Mathematics*, New York, McGraw-Hill, 1951, p. 509.
14. Dow, P.C. et.al., "Dynamic Stability of a Gravity Gradient Stabilized Satellite Having Long Flexible Antennas" presented at AIAA Guidance and Control Specialists Conference, Seattle, Washington, Aug. 15-17, 1966.